JACS Au
AN OPEN ACCESS JOURNAL OF THE AMERICAN CHEMICAL SOCIETY

pubs.acs.org/jacsau

Perspective

Design of Microstructure-Engineered Polymers for Energy and Environmental Conservation

Yazhen Xue,[†] Mengxue Cao,[†] Charles Chen, and Mingjiang Zhong*

Cite This: *JACS Au* 2023, 3, 1284−1300

Read Online

ACCESS | Metrics & More | Article Recommendations

ABSTRACT: With the ever-growing demand for sustainability, designing polymeric materials using readily accessible feedstocks provides potential solutions to address the challenges in energy and environmental conservation. Complementing the prevailing strategy of varying chemical composition, engineering microstructures of polymer chains by precisely controlling their chain length distribution, main chain regio-/stereoregularity, monomer or segment sequence, and architecture creates a powerful toolbox to rapidly access diversified material properties. In this Perspective, we lay out recent advances in utilizing appropriately designed polymers in a wide range of applications such as plastic recycling, water purification, and solar energy storage and conversion. With decoupled structural parameters, these studies have established various microstructure−function relationships. Given the progress outlined here, we envision that the microstructure-engineering strategy will accelerate the design and optimization of polymeric materials to meet sustainability criteria.

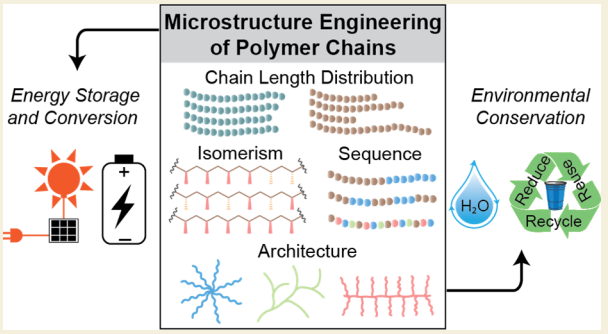

KEYWORDS: *Polymer Microstructures, Environmental Preservation, Energy Storage, Energy Conversion, Sustainability*

Designing new materials to solve energy and/or environmental crises have been actively pursued to meet the global sustainable development goals. Among a variety of material design strategies, microstructure engineering of polymeric materials provides a potent platform for rapid discovery of next-generation materials toward energy and environmental applications through readily accessible feedstocks. This strategy relies on the inherent dependence of polymer properties on their microstructures, specifically referring to chain length distribution,[1−3] main chain regio-[4]/stereochemistry,[5] monomer or segment sequence,[6−8] and architecture[9−16] (Figure 1, top). It is worthwhile noting that the microstructure of polymer discussed here relates to the covalent arrangement of monomer residues in a macromolecular chain, which should be distinguished from the definition of microstructure in material science that describes the microscopic morphologies and phase behaviors of materials.[17] By microstructure engineering, it opens a convenient and economic way to access polymers with broadly tunable functions without compositional variance. The recent development of precision synthesis techniques has promoted the preparation of microstructure-engineered polymers for applications in environmental preservation, such as plastic re/upcycling, water purification, and fouling-resistant surface fabrication, and for energy conversion and storage, such as flexible optoelectronics, dielectric materials, and solid-state electrolytes in batteries (Figure 1, bottom).

This Perspective sets out to highlight these recent advances with a particular emphasis on the microstructure−property relationships that form the foundations or rationales for each material design. We selected examples from studies that decoupled the microstructure parameters and isolated their impacts on the polymer functions and the resulting material performance. The influence of microstructure parameters on general polymer properties such as thermomechanical properties, morphologies, and processability that were previously reviewed[18−21] are not discussed here unless they are directly related to energy and environmental applications. While advancements in precision polymer synthesis are prerequisite tools for microstructure engineering, we will avoid repeating discussion on detailed synthetic procedures. In this Perspective, we hope to provide readers with insights into the design and optimization of polymeric materials to meet sustainability criteria.

Received: February 16, 2023
Revised: April 17, 2023
Accepted: April 17, 2023
Published: April 27, 2023

https://doi.org/10.1021/jacsau.3c00081
JACS Au 2023, 3, 1284−1300

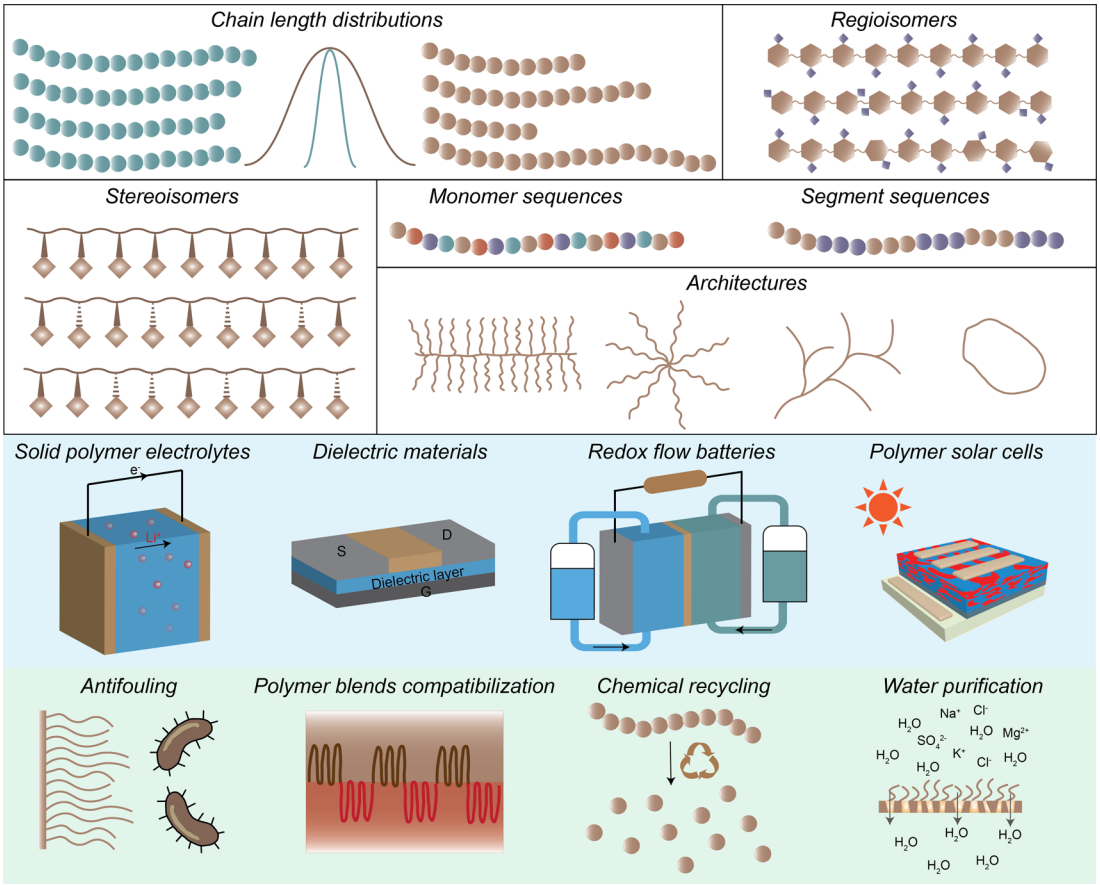

Figure 1. Overview of the polymer microstructure-engineering for the applications in energy and environmental conservation.

CHAIN LENGTH DISTRIBUTION

Synthetic polymers are usually made as mixtures of macromolecular chains with different lengths. The distribution of chain length or molecular weight of the mixtures dictates the ensemble polymer properties collectively contributed by each chain, where the individual chain behaviors are dependent on chain length.[1,2] While the breadth, shape, and symmetry of the distribution were each found essential for certain properties, e.g., assembly behaviors of block copolymers in bulk and solution,[20−28] rheological and mechanical properties,[29−33] and morphology of polymer-grafted-nanoparticle aggregates,[34−36] the dispersity index ($Đ$), i.e., the ratio of weight- and number-average molecular weights (M_w/M_n), is often adopted to roughly describe the distribution. Over the past decades, the development of precision synthesis methods, such as controlled/living polymerizations[37,38] and iterative synthesis,[39−41] and advanced separation[42−44] techniques promoted the ability to prepare polymers with controlled molecular weight and dispersity. Discrete ($Đ$ = 1.0) or low dispersity ($Đ$ < 1.2) polymers with eliminated or reduced structural heterogeneity were used to probe molecular weight−property relationships; on the other end, high dispersity or multimodally distributed polymers with mixed chain conformations were found to display superior performance in certain environmental applications, e.g., antifouling[45] and membrane modification.[46]

Antifouling surfaces based on physicochemical property changes in response to environmental alterations were designed using silicon wafers covalently grafted with pH-responsive poly(acrylic acid) (PAA).[45] Poly(*tert*-butyl acrylate) (P*t*BA) brushes with disparate dispersities were first obtained by surface-initiated atom transfer radical polymerization of *tert*-butyl acrylates with varied amount or stoichiometry of catalytic copper complexes.[47] Quantitative hydrolysis of P*t*BA side groups resulted in PAA brushes immobilized on a silicon surface. A nonuniform brush with a dispersity of 1.95 contained shorter PAA chains that were compressed and embedded by the surrounding longer PAA chains with extended conformations and enhanced freedom of movement[48,49] (Figure 2a). Stretching of these longer chains in

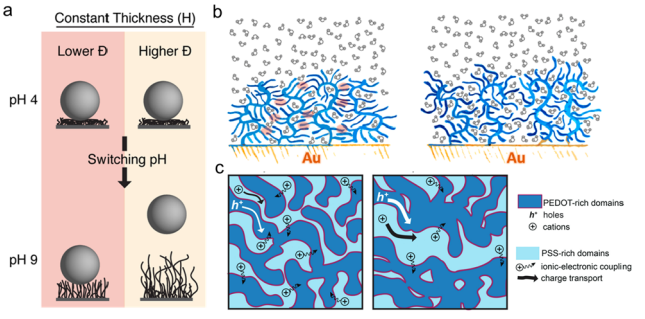

Figure 2. (a) Removal of *Staphylococcus epidermidis* on PAA modified surfaces. Reproduced from ref 45. Copyright 2017 American Chemical Society. (b) Hydration of polymer brush modified surfaces based on mono- (left) and polydisperse (right) side chains. Reproduced from ref 46. Copyright 2021 American Chemical Society. (c) Proposed mechanism for hole/electron transport in PEDOT:PSS with narrow (left) and broad dispersities (right). Reproduced with permission from ref 59. Copyright 2022 Royal Society of Chemistry.

https://doi.org/10.1021/jacsau.3c00081
JACS Au 2023, 3, 1284−1300

response to pH increase resulted in a film thicker than the uniform brush ($Đ$ = 1.33) with comparable average chain length, leading to more efficient detachment of *Staphylococcus epidermidis* at pH 9.

Graft polymers constructed by covalently tethering polymeric side chains to a linear main chain polymer can access diverse properties by tuning their chain lengths distributions.[11] For instance, graft copolymers with polydisperse side chains were employed to modify nanofiltration membranes to enhance water permeation flux and mitigate bio/organic fouling.[48−53] The graft copolymers synthesized by reversible addition−fragmentation chain transfer polymerization of polydisperse oligo(2-ethyl-2-oxazoline) methacrylate monomers exhibited 9% higher hydration and more effective lubrication than the monodisperse analogs with similar grafting densities.[46] The steric repulsion of longer side chains diminished polymer−polymer interactions, creating room for water molecule penetration and forming more hydrated membrane surfaces (Figure 2b).[54,55]

Blending dissimilar polymers to form composite materials is an industrially important strategy to integrate multiple functions and enhance material performance.[56−58] Recent studies showed that tuning polymer dispersity can also improve the performance of materials based on polymer blends.[59] The mixture of poly(3,4-ethylenedioxythiophene) (PEDOT) and poly(styrene sulfonate) (PSS) has been extensively studied in a variety of energy devices due to its optical transparency, chemical stability, solution processability, and desirable mixed electron-/ion-conductivity.[60−62] A PEDOT:PSS composite material with high dispersity PSS ($Đ$ = 1.7) exhibited approximately six times improved charge mobility and eight times higher transconductance in an organic electrochemical transistor compared to the composite containing low dispersity PSS ($Đ$ = 1.1). The mechanism of this dispersity-enhanced performance was attributed to the increase of structural heterogeneity resulting from the high dispersity PSS homopolymers. Enlarged PEDOT and PSS-rich domains facilitated hole and cation transport, respectively (Figure 2c, right). The low dispersity analogs featured homogeneously percolating ion- and electron-transport domains with larger interfacial areas (Figure 2c, left). Approximately 1.5 times higher volumetric capacitance were found in these materials due to stronger ion-electron coupling, making them advantageous in supercapacitor and battery applications.[63]

REGIOISOMERS

Polymers with designed regiochemistry of pendant substituents can be synthesized through copolymerization of regioisomeric monomers[4,64] or homopolymerization during which the unimonomeric units are enchained via various regioselective pathways.[65−67] In contrast to polymers in which the relatively flexible main chain conformation diminishes the impact of regiochemical heterogeneity on polymer morphology, the regioselective arrangement of the substituents profoundly influences chain packing and related properties of semicrystalline polymers such as conjugated polymers (CPs). (Semi)-conducting CPs serve in photovoltaic devices as light absorbers, electron donors/acceptors, or charge transport layers to assist the conversion of solar energy to stored electricity.[68,69] Complementing the prevailing strategy of designing novel CP monomers to improve the device efficiency, regioselective polymerizations were developed to synthesize high-performance CPs with controlled regioregularity (RR). Poly(3-hexylthiophene)s (P3HTs) represent an important class of solvent-processable CPs with easily tunable molecular weight, dispersity, and RR, where the degree of RR is quantified by the fraction of head-to-tail linkages of 3-hexylthiophene repeat units. With consistent molecular weights and processing conditions, high RR P3HTs tend to undergo more ordered chain packing to form microcrystalline lamellae that promote stronger intra- and interplane orbital coupling and charge transfer (Figure 3a).[70] The combination of P3HT

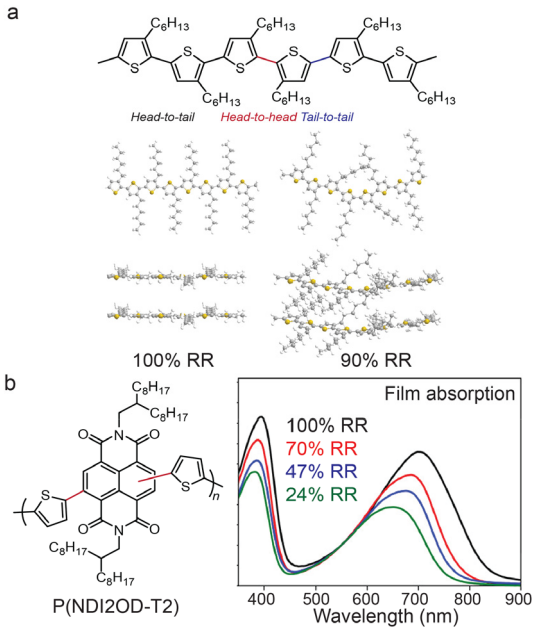

Figure 3. (a) Energy-minimized molecular structures of P3HTs with 100% and 90% RR. (b) Absorption spectra of 100%, 70%, 47%, and 24% RR CP thin films. Reproduced from ref 78. Copyright 2017 American Chemical Society.

electron donors and 1-(3-methoxycarbonyl)-propyl-1-phenyl-(6,6) C61 (PCBM) electron acceptors has been demonstrated in bulk heterojunction (BHJ) solar cells for efficient photocurrent generation.[71] Benefiting from the RR-enhanced optical absorption and charge transport, the blends containing P3HT of 95.2% RR displayed two times larger short-circuit current density and three times higher power conversion efficiency compared to the blends with 90.7% RR P3HTs.[72] Application of regioregular CPs in stretchable electronics is however limited by their reduced mechanical compliance due to the rigid chain packing. Introducing regioirregular amorphous CPs to regioregular CPs through physical blending[73] or covalent block copolymer formation[74] was adopted to achieve the desired mechanical performance.

Donor−acceptor (D−A) CPs synthesized from alternating copolymerization of donor and acceptor monomers allow for the customization of optoelectronic properties by separately engineering the two monomers.[75,76] A wide range of electron-rich and electron-deficient D−A CPs were designed for hole or electron stabilization to achieve the control over bandgap and energy levels. CPs with regio-varied connection of D−A units were synthesized by copolymerizing 5,5′-bis(trimethylstannyl)-2,2′-bithiophene (T2-Sn) with a mixture of *N*,*N*′-bis(2-octyldodecyl)-2,6- and -2,7-dibromonaphthalene-1,4,5,8-bis(dicarboximide)s (NDI2OD-2,6Br$_2$ and NDI2OD-2,7Br$_2$) at

https://doi.org/10.1021/jacsau.3c00081
JACS Au 2023, 3, 1284−1300

different feed ratios through Stille coupling reactions (Figure 3b).[77] Herein, RR describes the fraction of 2,6-linkages connecting T2 and NDI2OD units. With decreasing RR, chains exhibited a reduced tendency to aggregate in solutions and thin films. All-polymer solar cells were fabricated using these n-type CPs and poly[5,5′-bis(2-butyloctyl)-(2,2′-bithiophene)-4,4′-dicarboxylate-*alt*-5,5′-2,2′-bithiophene] (PDCBT) as the donor material. Solar cells with 47% RR CPs displayed a 3-fold increase in the power conversion efficiency compared to those with 100% RR CPs.[78] The n-type CPs which aggregated less resulted in limited disturbance to the crystallization of PDCBTs during the solvent blending process, increasing the optical absorption and photocurrent generation.[79]

Polymers with intrinsic microporosity (PIMs) made from inefficiently packed rigid ladder-like chains can be solvent-processed into membrane materials for gas and water purification.[80] The impacts of regio-isomerism on chain packing, fractional free volumes, and related separation performance were investigated.[81−83] Similar to the synthesis of regioisomeric D−A CPs, norbornyl bis-benzocyclobutene-containing Tröger's base PIMs with dissimilar main chain regioregularities were respectively prepared from two regioisomers obtained via catalytic arene-norbornene annulation (CANAL)[84,85] of 3-bromo-2-methylaniline and norbornadiene (Figure 4). Compared to the *anti*-isomers with a similar

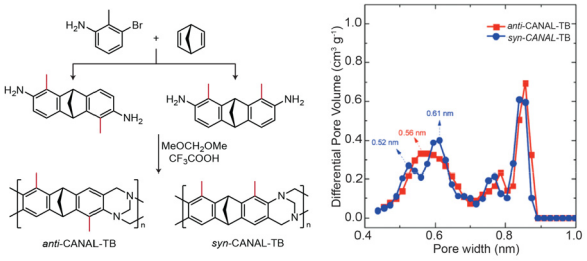

Figure 4. Synthetic route to *syn*- and *anti*-CANAL-TB and their pore size distributions. Reproduced with permission from ref 81. Copyright 2022 Royal Society of Chemistry.

thickness, the *syn*-isomers with pendent methyl groups residing on the same side of the main chains exhibited 6−14% higher permeability and 7% higher selectivity in H_2/CH_4 separation. This difference was ascribed to both a higher fractional free volume and formation of smaller ultramicropores (*ca.* 0.5 nm) in the *syn*-isomers.[81]

STEREOISOMERS

Studies on stereoisomeric polymers were formerly motivated by the strong dependence of polymer crystallinity and associated thermomechanical properties on their main chain stereoregularity. Polymers with broadly tuned thermomechanical properties[5] and processability[86] have been industrially produced via stereocontrolled polymerizations of a small set of monomers.[87,88] This facile strategy allows access to polymers with improved properties without varying composition and inspired polymer scientists to find pathways to address the growing concerns associated with the lack of reuse of consumer plastics and their negative impact on the environment and human health upon end-of-life disposal. As one of the most abundantly produced polyolefins, polypropylene (PP) is synthesized with tunable thermomechanical properties by engineering the relative stereochemistry of adjacent main chain stereogenic carbon centers, also known as tacticity. The crystallinity of PP decreases following the order of isotactic PP (*i*PP), syndiotactic PP (*s*PP), and atactic PP (*a*PP), where adjacent pendent methyl groups are arranged in a *meso*, *racemo*, and stereoirregular configuration, respectively.[89] Forming a sustainable recycling loop of plastics often requires the development of efficient deconstruction chemistries for naturally nondegradable polymers. Hydrogenolysis of *a*PPs, *i*PPs, and *s*PPs with similar molecular weights and dispersities was conducted, and substantially different low molecular weight products were obtained depending on the tacticity.[90] The liquid products of *a*PPs and *s*PPs were similar in size and had a narrow size distribution, whereas the products of *i*PP were significantly smaller and more broadly distributed. The higher chain mobility of *i*PP in the melt state indicated by its greater diffusion constant than *a*PP or *s*PP melts facilitated the mixing of polymer chains and catalysts, resulting in a higher chain scission efficiency.[91] Additional experimental evidence is needed to provide a thorough explanation for this degradation and product release process.

Synthesizing sustainable alternatives for naturally nondegradable plastics from renewable feedstock monomers is one of major approaches to solving the plastic crisis.[92−94] As one of the most widely studied sustainable plastics, polylactides (PLAs) received limited applications due to its yet-to-be-improved plastic properties and related tunability.[95] Through ring opening polymerizations (ROPs) of diastereomerically pure lactides and rational catalyst design for stereospecific ROP of *rac*-lactide, iso-, syndio-, and heterotacticity enriched PLAs were prepared.[96,97] Syndiotactic PLA showed the lowest intrinsic and melt viscosity in rheological studies. Iso- and heterotactic PLAs exhibited strain-hardening behaviors originating from crystalline domains formed through stereocomplexation of L- and D-LA segments.[98] Poly(β-hydroxybutyrate) (PHB) is another type of bioderived polyesters with pendent methyl groups. Extensive efforts have been devoted to the scalable synthesis of high molecular weight isotactic PHB since its biodegradability and thermomechanical properties that are comparable with commodity *i*PP.[99] The amorphous atactic PHB and semicrystalline syndiotactic PHB were also synthesized,[100−102] and blending these PHB stereoisomers provides a convenient way to tune the thermomechanical properties and degradability of the resulting materials.[103,104]

In addition to the impact on mechanical performance, the stereoisomerism has also been taken into consideration in the deconstruction kinetics as the crystalline phase impedes polymer degradation through various mechanisms.[105] For instance, compositionally identical polyurethanes (PUs) synthesized respectively from two stereoisomeric sugar-derived monomers, i.e., isoidide (II) and isomannide (IM) (Figure 5a), exhibited drastically different degradation rates.[106] The strong intramolecular hydrogen bonding ascribed to the *exo-exo* configuration resulted in predominantly crystalline phase in II-PUs, while the *endo*−*endo*-configurated IM-PU was amorphous. II-PU degraded slower than IM-PU under basic conditions as the base and water molecules that facilitated the degradation had restricted transport in the crystalline domains. On the other hand, the semicrystallinity provided II-PU with stiffness and ductility comparable to high-density polyethylene (PE), while the amorphous IM-PU formed a more mechanically compliant elastomer. Accelerating degradation while maintaining the desired mechanical properties of II-PU was achieved through blending II-PU with IM-PU

https://doi.org/10.1021/jacsau.3c00081
JACS Au 2023, 3, 1284−1300

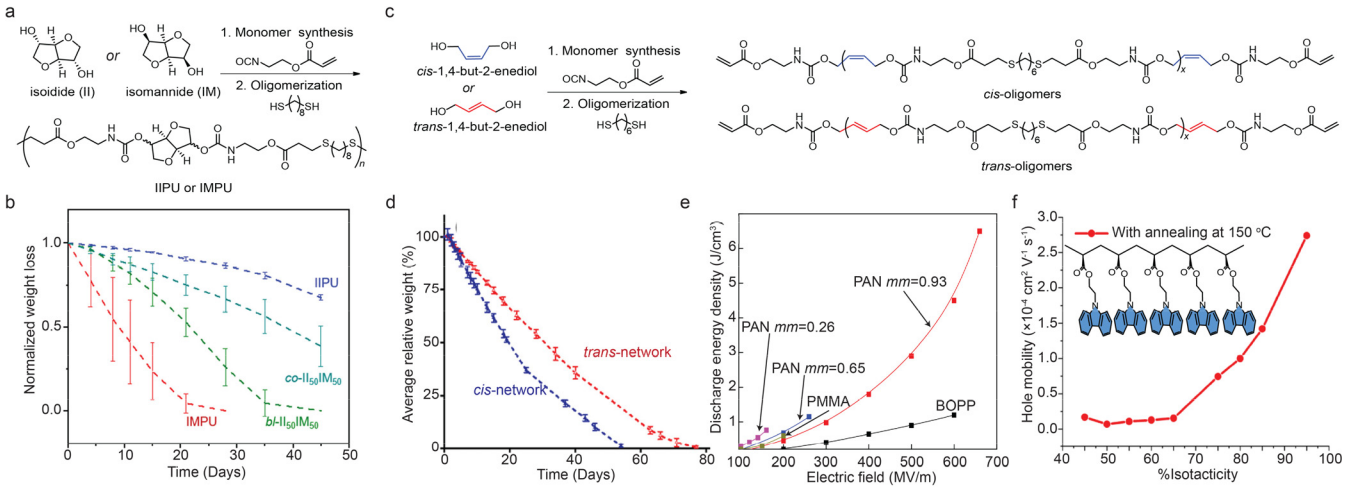

Figure 5. (a) Chemical structures of IIPU and IMPU. Reproduced from ref 106. Copyright 2022 American Chemical Society. (b) Degradation curves of IIPU, IMPU, the blends and block copolymers of IIPU and IMPU. Reproduced from ref 106. Copyright 2022 American Chemical Society. (c) Synthetic route to the *cis*- and *trans*-oligomer precursors of the photoset materials. Reproduced from ref 107. Copyright 2021 American Chemical Society. (d) Degradation curves of *cis*- and *trans*-networks in basic solutions. Reproduced from ref 107. Copyright 2021 American Chemical Society. (e) Energy densities of dielectric films fabricated from PAN with various fractions of *meso*−*meso* triads(*mm*); the performance of BOPP and isotactic PMMA were included for comparison. Reproduced from ref 114. Copyright 2020 American Chemical Society. (f) Tacticity-dependent hole mobility in PVCs. Reproduced from ref 118. Copyright 2021 American Chemical Society.

(Figure 5b). The degradation kinetics were also studied in photo-cross-linked polymer networks containing *cis*- or *trans*-isomeric vinyl units.[107] Polyester-based network precursors with defined main chain double bond configurations were synthesized from *cis*- or *trans*-1,4-but-2-enediol, 2-isocyanatoethyl acrylate, and 1,6-hexanedithiol (Figure 5c), and UV-cross-linking was applied to generate the polymer networks. Similar to polybutadiene rubbers,[108] the *cis*-network possessed less compact chain packing and reduced crystallinity, leading to faster hydrolytic degradation in basic solution due to the greater water molecule penetration for ester bond hydrolysis (Figure 5d).

Engineering tacticity in vinyl polymers also creates more opportunities for their extensive applications in energy devices. Polymer-based dielectric materials are widely applied because of their good processability and tunable thermomechanical properties. Designing dielectric polymers with high energy density, high charge−discharge efficiency, and low dielectric loss presents a major challenge in current research.[109] The energy density U_e can be expressed as a function of the relative dielectric constant ε_r and breakdown strength E_b of the dielectric materials as illustrated in the equation, $U_e = 0.5\varepsilon_0\varepsilon_r E_b^2$. While the ε_r is related to the polarity of the polymers, E_b is strongly dependent on the packing structure of polymer chains. Biaxially oriented *i*PP (BOPP) films with uniformly oriented *i*PP crystalline domains are widely used as film capacitors.[110,111]The dense and compact chain packing with reduced free volumes between the polymer chains minimizes the collisions with the high energy mobile charges that transport in the fabricated films, thereby increasing the electrical breakdown voltage.[112] In addition to BOPP, studies on polymers with higher ε_r such as poly(methyl methacrylate) (PMMA) (ε_r = 3.0) and polyacrylonitrile (PAN) (ε_r = 3.2) have shown that the tacticity engineering is a generalizable strategy to improve the dielectric performance. Isotactic PMMA exhibited the highest E_b among the three PMMA stereoisomers, and was more than three times higher than that of atactic PMMA.[113] PAN with higher degree of isotacticity exhibited enhanced breakdown threshold, energy density, and charge−discharge efficiency and reduced dielectric loss (Figure 5e). This isotacticity-enhanced performance could be attributed to the hindered reorientation of the cyano groups in the closely packed isotactic chains.[114]

Vinyl polymers with electroactive pendent groups have been designed as a class of nonconjugated electroactive polymers. These polymers hold several advantages over CPs, such as improved solution processability, facile polymerization processes, and easier modification through pendant group functionalization.[115] Charge transport in the nonconjugated polymers such as poly(vinyl carbazole) (PVC) arises from long-range $\pi-\pi$ stacking of the neighboring carbazole groups, the degree of which is dictated by the tacticity. In isotactic PVC, the pendant groups adopted a totally eclipsed conformation, forming excimers that require lower excitation energies. In contrast, partially overlapped excimers formed in syndio- or atactic PVCs due to unoptimized pendant group arrangements. This conformational difference led to different fluorescent emissions of PVC.[116,117] Studies on their electrical properties indicated a positive correlation between hole mobility and the degree of isotacticity. When the fraction of *meso* diads increased from 45% to 95%, the hole mobility was improved by an order of magnitude, with the highest value of 2.74×10^{-4} cm^2 V^{-1} s^{-1} being comparable to CPs such as P3HTs. (Figure 5f).[118−121]

SEQUENCE

The diverse biomacromolecular functions enabled by precisely controlled monomer sequences motivated polymer chemists to make efforts to develop methodologies to prepare sequence-defined synthetic analogs to elucidate the sequence-structure−function relationships.[6,8,122] Strategies such as solid/liquid-phase synthesis,[7,123−125] templated polymerization,[126−131] single unit monomer insertion[132,133] and iterative exponential growth[134,135] were explored to achieve monomer sequence control in oligomeric or low molecular weight polymeric products. Sequence-defined polyphosphates, poly(alkoxyamine

https://doi.org/10.1021/jacsau.3c00081
JACS Au 2023, 3, 1284−1300

amides), and polyurethanes hold promise in secure data storage as molecular barcodes and QR codes.[136−140] Discrete block copolymers containing immiscible segments (e.g., PLA and polydimethylsiloxane (PDMS)[141]) provide an ideal model for phase separation studies to resolve the impact of atomic-level alteration on phase behaviors.

Sequence-defined antifouling polymers were developed as effective coating materials to modify the interactions between surfaces and fouling components such as bacteria and proteins. Peptoids, or poly(*N*-substituted glycine)s, were designed as peptidomimetic polymers and provided a versatile platform to incorporate diverse functional groups in a sequence-defined manner.[142,143] A series of zwitterionic peptoids with unchanged charge density yet varied sequence arrangements of amino and carboxylic side groups were synthesized from lysine- and glutamic acid-type monomers (Figure 6a). Neutral

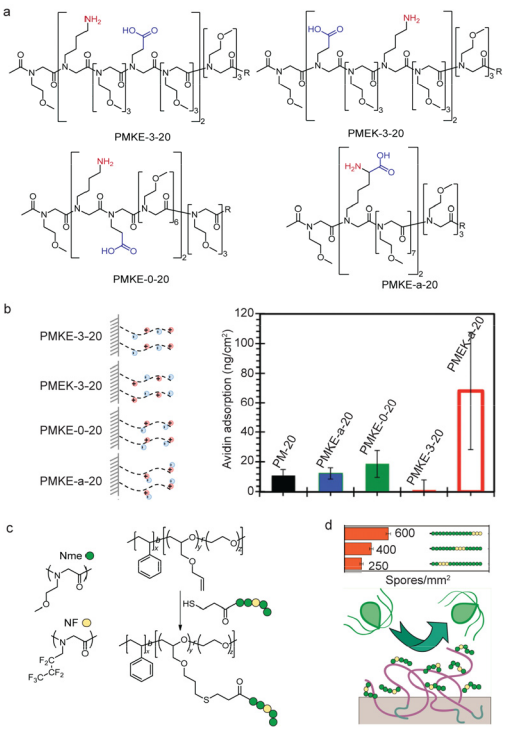

Figure 6. (a) Chemical structures of antifouling zwitterionic peptoids. Reproduced with permission from ref 144. Copyright 2015 John Wiley and Sons. (b) Schematics of the grafted charge arrangement of the zwitterionic peptoids and their avidin adsorption profiles (PM-20 stands for the neutral peptoids as a control). Reproduced with permission from ref 144. Copyright 2015 John Wiley and Sons. (c) Chemical structures of PS-*b*-P(EO-*co*-AGE) grafted with sequence-defined peptoid side chains. Reproduced from ref 145. Copyright 2014 American Chemical Society. (d) Spore settlement density on silicon surfaces modified with graft copolymers. Reproduced from ref 145. Copyright 2014 American Chemical Society.

N-(2-methoxyethyl)glycine monomers were incorporated to control the distances between the oppositely charged side groups. After grafting the peptoids onto a TiO_2 substrate of a prototypical biomedical device by leveraging their dihydroxyphenylalanine-containing pentapeptide chain ends, the modified the surface was exposed to a solution of avidin, i.e., a positively charged protein at neutral pH. Peptoids bearing positively charged terminal residues inhibited avidin adsorption more effectively via electrostatic repulsion than peptoids with a reverse sequence of the monomers. At the same time, the long distance between the oppositely charged groups also played an important role in mitigating the protein fouling due to the sufficient separation of the charges (Figure 6b).[144] In a graft copolymer containing polystyrene-*b*-poly(ethylene oxide-*co*-allyl glycidyl ether) block copolymer backbones, *N*-(2-methoxyethyl)glycine and *N*-(heptafluorobutyl)glycine derived peptoid side chains were tethered to the glycol-based block (Figure 6c). When the copolymer was deposited on silicon wafers, the peptoid-grafted block was exposed on the film surface due to the lower surface energy of fluorinated residues, while the polystyrene block was forced to reside close to the substrate. When the *N*-(heptafluorobutyl)glycine units were moved from the outer edge of the peptoid to a position close to the backbone, the amount of glycol residues exposed to the surface increased, leading to a more hydrophilic surface and lower settlement of *Ulva linza* spores (Figure 6d).[145]

The concept of varying monomer sequence to obtain targeted material properties was extended to engineering block or segment sequence in multiblock copolymers toward applications requiring large-scale production.[146] PE/*i*PP-containing multiblock copolymers with fixed block lengths were designed as compatibilizers to improve the interfacial adhesion of high density PE (HDPE)/*i*PP blends. The poor mechanical properties resulting from the immiscibility of HDPE and *i*PP were significantly improved through the block copolymer assisted interfacial adhesion, providing a sustainable solution for recycling the worldwide produced mixed HDPE/*i*PP waste. HDPE/*i*PP blends containing tetra- or hexablock copolymers of alternating PE and *i*PP segments exhibited significantly larger elongation-at-break in tensile tests than the system based on diblock copolymers with comparable PE/*i*PP segment lengths. The multiblock compatibilizers phase-segregated with their corresponding homopolymers and resided at the interfaces between the macrophase-separated HDPE and *i*PP domains, forming entanglement loops that effectively stitched together the homopolymers in the melts and cocrystallized upon cooling. This phase segregation led to a reduction in the average *i*PP droplet size from 2.2 to 0.55 μm in the HDPE matrix as shown by TEM imaging (Figure 7).[147,148] These unique interfacial interactions between the multiblock compatibilizers and HDPE/*i*PP blends accounted for the efficient stress transfer between phases and the subsequent mechanical enhancement of the blends.

Inspired by the properties of linear $(AB)_n$ alternating multiblock copolymers, copolymers with periodically inserted single functional units were synthesized via step-growth polymerizations. These periodically functionalized polymer structures were found to be beneficial for applications in energy storage capacitors, stretchable electronics, and solid-state polyelectrolytes.[149,150] For example, copolymers with PE main chains bearing carboxylic acid units inserted every 21 carbons were synthesized from hydrogenation of polymer precursors obtained from acyclic diene metathesis of protected carboxylic acid functionalized dienes. Two sets of scattering reflections were observed in the 2D X-ray scattering patterns of these polymers, corresponding respectively to the inter-PE chain distance and intergroup distance between adjacent dimeric carboxylic acids formed in the crystalline domains (Figure 8a).[151] Replacing the carboxyl groups with more hygroscopic sulfonic acids could allow the polymers to function as proton exchange membranes for fuel cell applications (Figure 8b). Microphase separation between PE

https://doi.org/10.1021/jacsau.3c00081
JACS Au 2023, 3, 1284−1300

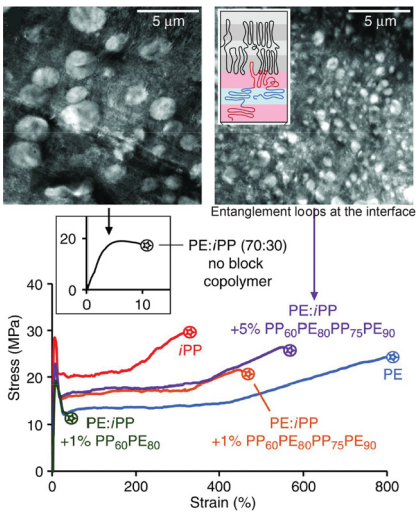

Figure 7. Mechanical enhancement of HDPE/*i*PP blends by the tetrablock PE/*i*PP copolymers. Reproduced with permission from ref 147. Copyright 2017 The American Association for the Advancement of Science.

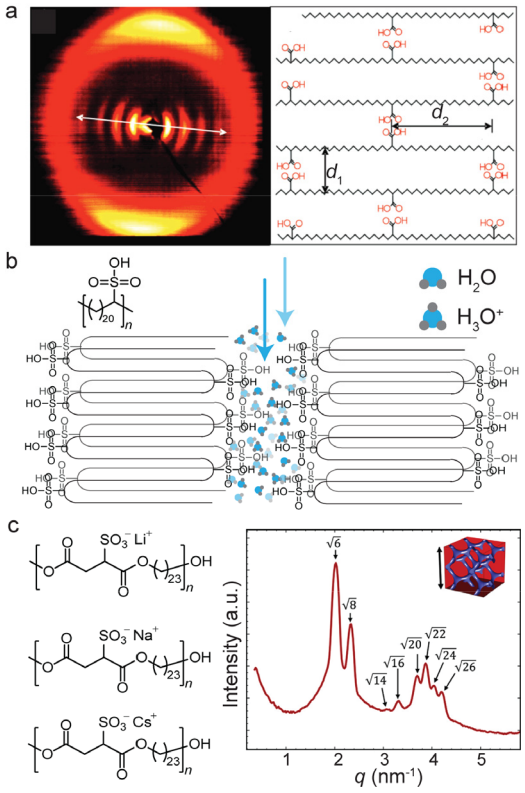

Figure 8. (a) Schematic of carboxylic acid dimer arrangement within the PE crystalline domain and the corresponding X-ray scattering patterns. Reproduced from ref 151. Copyright 2007 American Chemical Society. (b) Proton transport nanochannel formation in the copolymers with PE main chains periodically inserted with sulfonic acid units. (c) Single ion conductors with PE main chains periodically inserted with lithium, sodium, and cesium sulfonate units and their gyroid morphologies. Reproduced from ref 153. Copyright 2020 American Chemical Society.

and sulfonic groups formed nanochannels for proton transport. Both experiment and simulation results showed that the ordered layered structure enhanced water diffusion relative to the tortuous channels of an amorphous polymer.[152] Cation exchange of protons with Li^+, Na^+, Cs^+, or NBu_4^+ was carried out for the synthesis of single-ion conducting polymers. The precisely segmented PE main chains of these solid-state polyelectrolytes phase-separated with the evenly spaced sulfonate groups, resulting in ordered ionic aggregates. The morphologies transitioned upon heating from a layered or cylindrical phase to bicontinuous gyroids, providing improved ion conductivity due to the formation of ion-percolated structures for efficient charge transport (Figure 8c).[153]

ARCHITECTURE

Architecture-engineered polymers beyond linear chains have emerged as a class of important materials in a broad spectrum of applications. In particular, branched polymers, including randomly (hyper)branched or dendritic polymers,[15,16,154,155] bottlebrush-like or graft polymers,[156−163] and star-shaped polymers,[164] have been synthesized with high precision[10−12,14,165−171] and extensively studied to leverage the unique properties arising from their nonlinear intramolecular connections in the context of advanced environmental and energy materials. Although these different branched polymers afford properties that cannot be readily achieved in their linear counterparts, such as low viscosity, high end-group functionality, and reduced chain entanglement, the forms of intermolecular connections, i.e., topologies, and the degree of branching must be precisely controlled to access target material performance in specific applications.

Various branched polymers have displayed potential advantages in antifouling applications.[172−198] An ABA-type triblock copolymer containing a lubricin-mimicking zwitterionic bottlebrush middle block was designed for antifouling surface modification (Figure 9a).[187,188] The two positively charged linear end blocks strongly absorbed to a silica surface through cooperative hydrogen bonding, electrostatic, and hydrophobic interactions, thereby erecting the side chains of the thoroughly hydrated middle block against the substrate surface to efficiently repel proteins and bacteria. A mixed-graft block copolymer (mGBCP)[11,199−201] with peptide backbone

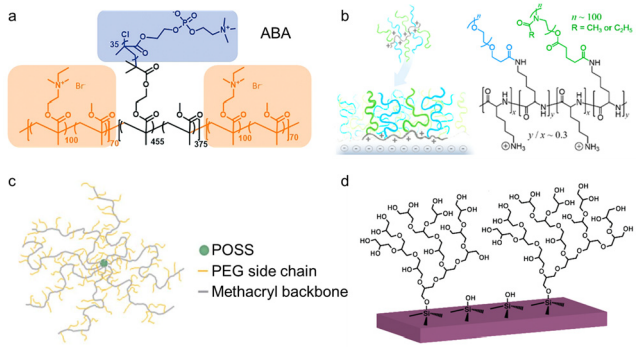

Figure 9. Branched polymers for antifouling applications. (a) ABA-type bottlebrush block copolymers with cation and zwitterion units. Reproduced with permission from ref 188. Copyright 2019 John Wiley and Sons. (b) Bottlebrush copolymers with randomly distributed PEO and poly(2-alkyl-2-oxazoline) side chains. Reproduced from ref 189. Copyright 2018 American Chemical Society. (c) Star-shaped polymers. Reproduced with permission from ref 191. Copyright 2012 Royal Society of Chemistry. (d) Hyperbranched polyglycerol. Reproduced from ref 198. Copyright 2014 American Chemical Society.

https://doi.org/10.1021/jacsau.3c00081
JACS Au 2023, 3, 1284−1300

and randomly distributed PEO and poly(2-alkyl-2-oxazoline) side chains also exhibited highly biopassive and lubricious features (Figure 9b).[189] Similar to the above-discussed ABA triblock copolymer, a vertical side chain orientation was obtained through the electrostatic adsorption of the positively charged backbone to the negatively charged surface. The mixed-graft copolymer architecture exhibited enhanced side chain hydration and suppressed aggregation of identical grafts, outperforming graft polymers singly grafted with either PEO or poly(2-alkyl-2-oxazoline). Star-shaped polymers with poly(poly(ethylene glycol) methyl ether methacrylate) arms were also synthesized as candidate antifouling coating materials (Figure 9c).[191] Compared to their linear analogs, SPs displayed a higher degree of hydration due to their stretched arms near the core, accompanied by a weaker interaction between the surfaces and the proteins.

Pressure-retarded osmosis (PRO) has garnered great attention as an efficient and scalable technique to harvest osmosis energy. However, fouling on PRO membranes reduces their lifetime and raises the maintenance cost, especially when a porous support layer is used. Hyperbranched polyglycerol (HPG) that was proven to be more thermally and oxidatively stable[202] as well as more biocompatible[203] than linear PEO was utilized to modify surfaces to enhance their fouling resistance (Figure 9d).[173,175,181,183,198] To evaluate the antifouling ability in PRO processes, HPG was grafted onto a poly(ether sulfone) hollow fiber membrane coated with polydopamine which covalently immobilizes thiol-functionalized HPG under oxidative conditions. Bovine serum albumin was added into the feed solution as a foulant in one dose and the water flux was monitored. HPG-grafted membrane experienced a lower level of flux decline compared to membranes grafted with linear PEO due to enhanced fouling resistance, and showed a higher level of recovery after membrane cleaning. Hyperbranched polymers with degradable branch junctions were designed in antifouling applications.[174,178,182,185] Degradation of these materials breaks them down to small molecules and oligomers that can be efficiently released, thereby reducing the negative environmental impacts from the polymeric coatings.

Nanofiltration membranes surface-modified with HBP also showed improved permselectivity in water purification compared to linear polymer based systems.[204−207] As an established modification strategy, positively and negatively charged polymers are alternately deposited to the membrane surface in a multilayer configuration stabilized through electrostatic interfacial adsorption. This layer-by-layer approach typically involves a labor-intensive procedure with 20 to 80 deposition steps to attain high ion-transport selectivity. Polyelectrolytes with improved efficiency for each individual layer were designed to reduce the number of layers and overcome the trade-off between membrane permeability and selectivity.[208] Hyperbranched polyelectrolytes (HPEs) possess a higher volumetric density of charged functionalities compared to the less conformationally compact linear polyelectrolytes (LPE), thereby enhancing the dynamic interactions with transporting ions. The hyperbranched architecture also renders maximal surface coverage without impeding ion transport through the internal voids of the polymers. In model systems constructed with positive poly(diallyldimethylammonium chloride) and negative sulfonated polyaryleneoxindole layers, a membrane with only one layer of negatively charged HPE exhibited similar selectivity and two times higher permeability compared to the membrane containing 10−20 layers of negatively charged LPE.[207] HPEs were also integrated into nanofiltration membranes by interfacial polymerization of HPE-based macromonomers.[209−213] Surface HPE formed through cross-linking reactions of hyperbranched poly(ethylene imide) and multifunctionalized acyl chlorides showed 2−5 times higher permeance and up to 1.5 times higher salt rejection than those composed of LPE derived from ethylenediamine or diethylenetriamine.[210] This improvement in selectivity arises from the large quantity of ion-interactive amine/ammonium functionalities immobilized in the active layer, while the internal voids created by the branched architecture preserve space to allow rapid ion transport and high membrane permeability. The simultaneous enhancement in both membrane selectivity and permeability was also observed in nanofiltration membranes based on star-shaped polyelectrolytes with similar structural features to HBPs.[214−216]

Branched polymers with richly functionalized chain ends grant them great potential in environmental sensing through signal amplification.[217−221] Hyperbranched polycarbosiloxanes were grafted from a resonant silica microcantilever, and their chain ends were functionalized with 4-(2-(4-(allyloxy)phenyl)-1,1,1,3,3,3-hexafluoropropan-2-yl)phenol sensing molecules that can recognize and absorb dimethyl methylphosphonate.[219] The hyperbranched architecture provided a large number of sensing sites while the quantity of grafting sites on the cantilever remained low, suppressing the parasitic frequency shift from the cantilever spring stiffening effect. With hyperbranched polymer-modified cantilevers, trace amounts of dimethyl methylphosphonate vapor down to 7.2 parts per billion was able to be detected due to the abundance of the sensing molecules.

Solid polymer electrolytes (SPEs) have been extensively studied as potential alternatives to liquid or gel electrolytes in lithium batteries with extended lifetime.[222−224] The flexible yet mechanically robust nature of SPEs addresses the safety issues caused by solvent leakage and lithium dendrite growth occurring in liquid electrolytes, and provides better electrode wettability compared to inorganic solid electrolytes. PEO is the most systematically studied SPE for Li^+ conduction due to its suitable Li^+ coordination behaviors and high dielectric constant.[225,226] However, the crystallinity of solid-state PEO reduces chain mobility and ion conductivity below its melting point (T_m), and therefore a high operating temperature ($T > T_m$) is often required to elevate the conductivity. Low molecular weight PEO generates crystallization-free melts at room temperature, but the viscoelastic liquid features disqualify these short-chain materials for SPE applications. Linking short PEO chains to form viscoelastic-solid graft polymers has proven to be an effective way to synthesize SPE with suppressed crystallization and increased ion conductivity.[227−239] Early efforts employed a graft-through method via free radical polymerization[230,231] or polycondensation[233] to synthesize PEO-grafted polymers which exhibited elevated Li^+ conductivity at room temperature. The structure−property relationship of a graft polyelectrolyte was established using precisely defined monodispersed polypeptoids with oligomeric ethylene oxide $(EO)_n$ side chains (Figure 10a).[234] Longer $(EO)_n$ (i.e., a larger n) side chains provided a higher conductivity due to the lower glass transition temperature (T_g).

Block copolymers derived from grafted PEO offer a way to enhance the mechanical strength via nanophase separa-

https://doi.org/10.1021/jacsau.3c00081
JACS Au 2023, 3, 1284−1300

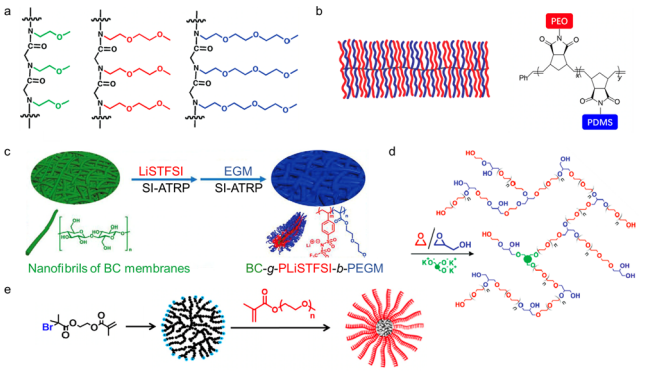

Figure 10. Branched polymers used as solid polymer electrolytes. (a) Polypeptoids with oligomeric ethylene oxide $(EO)_n$ side chains. Reproduced from ref 234. Copyright 2012 American Chemical Society. (b) Mixed-graft block copolymer. Reproduced with permission from ref 227. Copyright 2020 Elsevier. (c) Single-ion-conducting graft polymers with a hard cellulose backbone. Reproduced with permission from ref 239. Copyright 2021 John Wiley and Sons. (d) Hyperbranched random copolymers of EO and glycidol. Reproduced from ref 241. Copyright 2011 American Chemical Society. (e) Hierarchically branched polymers with a hyperbranched core and bottlebrush arms. This image reproduced from ref 240 is licensed under CC BY 4.0.

tion.[227,228] mGBCPs containing dissimilar side chains grafted on a linear backbone were designed as room-temperature solid lithium-ion conductors (Figure 10b).[227] The immiscible PEO and PDMS side chains undergo phase separation to form ordered nanostructures with the backbone lying at the interface of the two neighboring domains. By incorporating short PEO side chains with T_m below room temperature, mGBCP-based SPEs with room-temperature conductivity of up to 2.0×10^{-4} S/cm were synthesized. While these graft copolymers are derived from liquid-like PEO and PDMS side chains, the formation of bicontinuous phases percolated with nanostructurally defined interfaces resulted in a high modulus of the polymer electrolyte. Introducing rigid backbones, e.g., bacterial cellulose, provides an alternative way to improve the mechanical strength of a graft polyelectrolyte. A block copolymer containing a poly(lithium 4-styrenesulfonyl-(trifluoromethylsulfonyl) imide) (PLiSTFSI) and a poly(diethylene glycol monomethyl ether methacrylate) (PEGM) block was integrated as the side chain to forma single-ion-conducting SPE (Figure 10c).[239] The inherently stiff cellulose resulted in a high modulus of the polyelectrolyte even as an ultrathin film blended with plasticizers, while the soft $(EO)_2$-based side chains enabled the rapid ion transport. The cell fabricated from this polyelectrolyte demonstrated improved stability and an extended lifetime of 3300 h of lithium plating/stripping cycles.

Similar design principles were applied to inhibit crystallization for room-temperature SPEs by synthesizing hyperbranched or star-shaped PEO analogues.[240−250] Hyperbranched random copolymers of EO and glycidol exhibited a 100-fold higher ion conductivity than their linear counterparts.[241] The degree of branching was tuned by varying the feed ratio of comonomers, and 8 mol % glycidol was found to be sufficient to lower the crystallinity (Figure 10d). Further increases in glycidol content introduced additional hydroxyl terminal groups, forming hydrogen bonding interactions that impeded ionic motions. Higher-order hierarchical structures were designed to combine characteristics of different architectures. For example, a star-shaped polymer was synthesized from an EO-containing hyperbranched core, with PEO-grafted polymer arms (Figure 10e).[240] Such architecture provided a 20-fold higher conductivity than linear PEO with a similar molecular weight. Extension of the arms with linear PEOs further increased their moduli due to the physical cross-linking introduced by the crystallization.

Porous carbons with a high surface area, tunable pore size, stable material skeleton, and high conductivity are desirable electrode materials for batteries, supercapacitors, and electrocatalysis.[251−253] These materials can be synthesized through carbonization of nanostructured block copolymers containing a carbon precursor block and a sacrificial porogenic block.[254−258] Bottlebrush block copolymers with a PDMS-grafted block and a PEO-grafted block were coassembled with resol to form a body-centered cubic morphology with PDMS concentrated as discrete spheres in a PEO/resol continuous phase.[257] The PDMS domain was thermally degraded upon pyrolysis to yield porous carbons with pore sizes resembling the domain sizes of PDMS in the precursors. The densely grafted side chains led to extended bottlebrush conformation and increased the domain size. The domain size scaled linearly with the molecular weight of the bottlebrush block copolymer, providing precise and facile control over the pore size of resultant carbons through tuning the molecular weight of the parent polymers.

Redox flow batteries that circulate two redox-active liquid electrolytes, catholyte and anolyte, in a membrane-separated electrochemical cell, are critical in large-scale energy storage and delivering energy over a relatively long duration.[259,260] Their lifetime, however, can be compromised by crossover between catholytes and anolytes through the separator. Anchoring redox-active functionalities onto a polymer chain has been utilized to suppress the crossover, but the high concentration of the polymers needed for high capacity energy storage either exceeds the solubility of the polymers or results in high-viscosity catholyte and anolyte that raise operating costs and lower the round-trip efficiency.[261] On the contrary, branched polymers exhibit lower solution viscosity compared to their linear counterparts for similar density redox-active groups. For example, a bottlebrush polymer with poly(4-methacryloyloxy2,2,6,6-tetramethylpiperidin-1-oxyl) side chains was applied as the catholyte material.[262] The bottlebrush architecture not only allowed a high density of 2,2,6,6-tetramethylpiperidin-1-oxyl groups that facilitated the charge transfer and enhanced the capacity, but also created redox-active objects that could be size-excluded from the semipermeable membrane separator.

CONCLUSIONS AND OUTLOOK

Since Staudinger's seminal paper of *Über Polymerization* published a century ago,[263] the development of synthetic polymers has led to innovative discoveries in numerous fields. In this Perspective, we highlighted recent successes in designing microstructure-engineered synthetic polymers for potential energy and environmental applications. These successes benefited from a plethora of microstructure−property relationships established in fundamental polymer research based on precision synthesis, structure characterization, and property evaluation. The structural heterogeneity introduced by the shape and breadth of chain length distribution influences polymer properties that are dictated by chain conformations on surfaces or in bulk states. Increasing

https://doi.org/10.1021/jacsau.3c00081
JACS Au 2023, 3, 1284−1300

the degree of regio- or stereoregularity results in more compact chain packing and enhanced crystallinity, thereby altering polymers' properties and degradability. Sequence control in synthetic polymers, mimicking the biomacromolecules, facilitates the synthesis of multifunctional materials using a limited number of monomeric building blocks. Introducing different forms and degrees of branching to polymer chains offers greater structural tunability, creating a higher density of end groups and enabling the integration and independent manipulation of distinct functionalities. These general and facile microstructure-engineering strategies hold promise to address real world challenges associated with sustainability but there remains room for improvement. The trade-off between synthetic scalability and degree of precision in the microstructure control needs to be addressed in nearly all above-discussed applications. While the developed controlled or precision polymer synthesis methods have proved their power in creating materials to establish microstructure−property relationships, the optimal materials designed based on these relationships still require an industrially relevant synthetic route for scale-up. In addition to the concern regarding the limited scalability, microstructure-engineered polymers cannot be readily accessed by a broad scope of monomers. For instance, iso-/syndiotactic polymerizations of α-olefin are predominant in industrial plastic production but cannot be generalized to the tacticity control for other vinyl polymers, especially those synthesized from monomers with polar functionalities.[264] Therefore, the tacticity-dependent properties cannot be fully leveraged for the design of functional polymers.[265] Developing microstructure-controlled polymerizations for diverse functional monomers is one of the keys to broadening the utility of microstructure engineering. Future focuses in the topic can also be placed on those systems that lack systematic investigation due to either their difficulties in synthesis or characterization. For example, cyclic polymers that still cannot be synthesized in a controlled and scalable manner are not discussed in the Perspective, though these chain-end-free polymers have shown a series of unique properties such as compact packing,[266] reduced viscosity,[267−269] and improved hydration[270] that can be distinguished from the linear and branched chains in melts, solutions, and at interfaces.[13,271,272] Finding applications that take advantage of these properties remains underexplored in the energy and environmental fields.

AUTHOR INFORMATION

Corresponding Author

Mingjiang Zhong − *Department of Chemical and Environmental Engineering and Department of Chemistry, Yale University, New Haven, Connecticut 06511, United States;* orcid.org/0000-0001-7533-4708; Email: mingjiang.zhong@yale.edu

Authors

Yazhen Xue − *Department of Chemical and Environmental Engineering, Yale University, New Haven, Connecticut 06511, United States*

Mengxue Cao − *Department of Chemical and Environmental Engineering, Yale University, New Haven, Connecticut 06511, United States;* orcid.org/0000-0002-3964-4984

Charles Chen − *Department of Chemical and Environmental Engineering, Yale University, New Haven, Connecticut 06511, United States*

Complete contact information is available at: https://pubs.acs.org/10.1021/jacsau.3c00081

Author Contributions

†Y.X. and M.C. contributed equally.

Notes

The authors declare no competing financial interest.

ACKNOWLEDGMENTS

We thank National Science Foundation (CHE-1845184, DMR-2003875, CHE-2108681) for support of this work. M.Z. acknowledges the support through Camille Dreyfus Teacher-Scholar Award. M.C. was partly supported by the Robert M. Langer Fellowship at Yale University.

REFERENCES

(1) Gentekos, D. T.; Sifri, R. J.; Fors, B. P. Controlling Polymer Properties through the Shape of the Molecular-Weight Distribution. *Nat. Rev. Mater.* **2019**, *4* (12), 761−774.

(2) Whitfield, R.; Truong, N. P.; Messmer, D.; Parkatzidis, K.; Rolland, M.; Anastasaki, A. Tailoring Polymer Dispersity and Shape of Molecular Weight Distributions: Methods and Applications. *Chem. Sci.* **2019**, *10* (38), 8724−8734.

(3) Yin, R.; Wang, Z.; Bockstaller, M. R.; Matyjaszewski, K. Tuning Dispersity of Linear Polymers and Polymeric Brushes Grown from Nanoparticles by Atom Transfer Radical Polymerization. *Polym. Chem.* **2021**, *12* (42), 6071−6082.

(4) Kim, Y.; Park, H.; Park, J. S.; Lee, J.-W.; Kim, F. S.; Kim, H. J.; Kim, B. J. Regioregularity-Control of Conjugated Polymers: From Synthesis and Properties, to Photovoltaic Device Applications. *J. Mater. Chem. A* **2022**, *10* (6), 2672−2696.

(5) Worch, J. C.; Prydderch, H.; Jimaja, S.; Bexis, P.; Becker, M. L.; Dove, A. P. Stereochemical Enhancement of Polymer Properties. *Nat. Rev. Chem.* **2019**, *3* (9), 514−535.

(6) Yang, C.; Wu, K. B.; Deng, Y.; Yuan, J.; Niu, J. Geared Toward Applications: A Perspective on Functional Sequence-Controlled Polymers. *ACS Macro Lett.* **2021**, *10* (2), 243−257.

(7) Badi, N.; Lutz, J.-F. Sequence Control in Polymer Synthesis. *Chem. Soc. Rev.* **2009**, *38* (12), 3383−3390.

(8) Lutz, J.-F.; Ouchi, M.; Liu, D. R.; Sawamoto, M. Sequence-Controlled Polymers. *Science* **2013**, *341* (6146), 1238149.

(9) Polymeropoulos, G.; Zapsas, G.; Ntetsikas, K.; Bilalis, P.; Gnanou, Y.; Hadjichristidis, N. 50th Anniversary Perspective: Polymers with Complex Architectures. *Macromolecules* **2017**, *50* (4), 1253−1290.

(10) Blosch, S. E.; Scannelli, S. J.; Alaboalirat, M.; Matson, J. B. Complex Polymer Architectures Using Ring-Opening Metathesis Polymerization: Synthesis, Applications, and Practical Considerations. *Macromolecules* **2022**, *55*, 4200.

(11) Le, A. N.; Liang, R.; Zhong, M. Synthesis and Self-Assembly of Mixed-Graft Block Copolymers. *Chem. − Eur. J.* **2019**, *25* (35), 8177−8189.

(12) Li, Z.; Tang, M.; Liang, S.; Zhang, M.; Biesold, G. M.; He, Y.; Hao, S.-M.; Choi, W.; Liu, Y.; Peng, J.; Lin, Z. Bottlebrush Polymers: From Controlled Synthesis, Self-Assembly, Properties to Applications. *Prog. Polym. Sci.* **2021**, *116*, 101387.

(13) Haque, F. M.; Grayson, S. M. The Synthesis, Properties and Potential Applications of Cyclic Polymers. *Nat. Chem.* **2020**, *12* (5), 433−444.

(14) Khanna, K.; Varshney, S.; Kakkar, A. Miktoarm Star Polymers: Advances in Synthesis, Self-Assembly, and Applications. *Polym. Chem.* **2010**, *1* (8), 1171−1185.

(15) Zheng, Y.; Li, S.; Weng, Z.; Gao, C. Hyperbranched Polymers: Advances from Synthesis to Applications. *Chem. Soc. Rev.* **2015**, *44* (12), 4091−4130.

(16) Yates, C. R.; Hayes, W. Synthesis and Applications of Hyperbranched Polymers. *Eur. Polym. J.* **2004**, *40* (7), 1257−1281.
(17) Mercier, J.; Zambelli, G.; Kurz, W. *Introduction to Materials Science*; Elsevier, 2002.
(18) Matyjaszewski, K. Macromolecular Engineering: From Rational Design through Precise Macromolecular Synthesis and Processing to Targeted Macroscopic Material Properties. *Prog. Polym. Sci.* **2005**, *30* (8), 858−875.
(19) Nunes, R. W.; Martin, J. R.; Johnson, J. F. Influence of Molecular Weight and Molecular Weight Distribution on Mechanical Properties of Polymers. *Polym. Eng. Sci.* **1982**, *22* (4), 205−228.
(20) Kim, I.; Li, S. Recent Progress on Polydispersity Effects on Block Copolymer Phase Behavior. *Polym. Rev.* **2019**, *59* (3), 561−587.
(21) Lynd, N. A.; Meuler, A. J.; Hillmyer, M. A. Polydispersity and Block Copolymer Self-Assembly. *Prog. Polym. Sci.* **2008**, *33* (9), 875−893.
(22) Buckinx, A.; Rubens, M.; Cameron, N. R.; Bakkali-Hassani, C.; Sokolova, A.; Junkers, T. The Effects of Molecular Weight Dispersity on Block Copolymer Self-Assembly. *Polym. Chem.* **2022**, *13*, 3444.
(23) Gentekos, D. T.; Jia, J.; Tirado, E. S.; Barteau, K. P.; Smilgies, D.-M.; DiStasio, R. A.; Fors, B. P. Exploiting Molecular Weight Distribution Shape to Tune Domain Spacing in Block Copolymer Thin Films. *J. Am. Chem. Soc.* **2018**, *140* (13), 4639−4648.
(24) Lynd, N. A.; Hillmyer, M. A. Influence of Polydispersity on the Self-Assembly of Diblock Copolymers. *Macromolecules* **2005**, *38* (21), 8803−8810.
(25) Schmitt, A. L.; Repollet-Pedrosa, M. H.; Mahanthappa, M. K. Polydispersity-Driven Block Copolymer Amphiphile Self-Assembly into Prolate-Spheroid Micelles. *ACS Macro Lett.* **2012**, *1* (2), 300−304.
(26) Terreau, O.; Luo, L.; Eisenberg, A. Effect of Poly(Acrylic Acid) Block Length Distribution on Polystyrene-b-Poly(Acrylic Acid) Aggregates in Solution. 1. Vesicles. *Langmuir* **2003**, *19* (14), 5601−5607.
(27) Widin, J. M.; Schmitt, A. K.; Schmitt, A. L.; Im, K.; Mahanthappa, M. K. Unexpected Consequences of Block Polydispersity on the Self-Assembly of ABA Triblock Copolymers. *J. Am. Chem. Soc.* **2012**, *134* (8), 3834−3844.
(28) Zhang, C.; Vigil, D. L.; Sun, D.; Bates, M. W.; Loman, T.; Murphy, E. A.; Barbon, S. M.; Song, J.-A.; Yu, B.; Fredrickson, G. H.; Whittaker, A. K.; Hawker, C. J.; Bates, C. M. Emergence of Hexagonally Close-Packed Spheres in Linear Block Copolymer Melts. *J. Am. Chem. Soc.* **2021**, *143* (35), 14106−14114.
(29) Combs, R. L.; Slonaker, D. F.; Coover, H. W. Effects of Molecular Weight Distribution and Branching on Rheological Properties of Polyolefin Melts. *J. Appl. Polym. Sci.* **1969**, *13* (3), 519−534.
(30) Rosenbloom, S. I.; Fors, B. P. Shifting Boundaries: Controlling Molecular Weight Distribution Shape for Mechanically Enhanced Thermoplastic Elastomers. *Macromolecules* **2020**, *53* (17), 7479−7486.
(31) Rosenbloom, S. I.; Gentekos, D. T.; Silberstein, M. N.; Fors, B. P. Tailor-Made Thermoplastic Elastomers: Customisable Materials via Modulation of Molecular Weight Distributions. *Chem. Sci.* **2020**, *11* (5), 1361−1367.
(32) Tzoganakis, C.; Vlachopoulos, J.; Hamielec, A. E.; Shinozaki, D. M. Effect of Molecular Weight Distribution on the Rheological and Mechanical Properties of Polypropylene. *Polym. Eng. Sci.* **1989**, *29* (6), 390−396.
(33) Ye, X.; Sridhar, T. Effects of the Polydispersity on Rheological Properties of Entangled Polystyrene Solutions. *Macromolecules* **2005**, *38* (8), 3442−3449.
(34) Hui, C. M.; Pietrasik, J.; Schmitt, M.; Mahoney, C.; Choi, J.; Bockstaller, M. R.; Matyjaszewski, K. Surface-Initiated Polymerization as an Enabling Tool for Multifunctional (Nano-)Engineered Hybrid Materials. *Chem. Mater.* **2014**, *26* (1), 745−762.
(35) Wang, Z.; Yan, J.; Liu, T.; Wei, Q.; Li, S.; Olszewski, M.; Wu, J.; Sobieski, J.; Fantin, M.; Bockstaller, M. R.; Matyjaszewski, K. Control of Dispersity and Grafting Density of Particle Brushes by Variation of ATRP Catalyst Concentration. *ACS Macro Lett.* **2019**, *8* (7), 859−864.
(36) Conrad, J. C.; Robertson, M. L. Shaping the Structure and Response of Surface-Grafted Polymer Brushes via the Molecular Weight Distribution. *JACS Au* **2023**, *3*, 333.
(37) Braunecker, W. A.; Matyjaszewski, K. Controlled/Living Radical Polymerization: Features, Developments, and Perspectives. *Prog. Polym. Sci.* **2007**, *32* (1), 93−146.
(38) Grubbs, R. B.; Grubbs, R. H. 50th Anniversary Perspective: Living Polymerization—Emphasizing the Molecule in. *Macromolecules. Macromolecules* **2017**, *50* (18), 6979−6997.
(39) van Genabeek, B.; Lamers, B. A. G.; Hawker, C. J.; Meijer, E. W.; Gutekunst, W. R.; Schmidt, B. V. K. J. Properties and Applications of Precision Oligomer Materials; Where Organic and Polymer Chemistry Join Forces. *J. Polym. Sci.* **2021**, *59* (5), 373−403.
(40) van Genabeek, B.; de Waal, B. F. M.; Gosens, M. M. J.; Pitet, L. M.; Palmans, A. R. A.; Meijer, E. W. Synthesis and Self-Assembly of Discrete Dimethylsiloxane−Lactic Acid Diblock Co-Oligomers: The Dononacontamer and Its Shorter Homologues. *J. Am. Chem. Soc.* **2016**, *138* (12), 4210−4218.
(41) Schumm, J. S.; Pearson, D. L.; Tour, J. M. Iterative Divergent/Convergent Approach to Linear Conjugated Oligomers by Successive Doubling of the Molecular Length: A Rapid Route to a 128Å-Long Potential Molecular Wire. *Angew. Chem., Int. Ed. Engl.* **1994**, *33* (13), 1360−1363.
(42) Lawrence, J.; Goto, E.; Ren, J. M.; McDearmon, B.; Kim, D. S.; Ochiai, Y.; Clark, P. G.; Laitar, D.; Higashihara, T.; Hawker, C. J. A Versatile and Efficient Strategy to Discrete Conjugated Oligomers. *J. Am. Chem. Soc.* **2017**, *139* (39), 13735−13739.
(43) Lawrence, J.; Lee, S.-H.; Abdilla, A.; Nothling, M. D.; Ren, J. M.; Knight, A. S.; Fleischmann, C.; Li, Y.; Abrams, A. S.; Schmidt, B. V. K. J.; Hawker, M. C.; Connal, L. A.; McGrath, A. J.; Clark, P. G.; Gutekunst, W. R.; Hawker, C. J. A Versatile and Scalable Strategy to Discrete Oligomers. *J. Am. Chem. Soc.* **2016**, *138* (19), 6306−6310.
(44) Zhang, C.; Bates, M. W.; Geng, Z.; Levi, A. E.; Vigil, D.; Barbon, S. M.; Loman, T.; Delaney, K. T.; Fredrickson, G. H.; Bates, C. M.; Whittaker, A. K.; Hawker, C. J. Rapid Generation of Block Copolymer Libraries Using Automated Chromatographic Separation. *J. Am. Chem. Soc.* **2020**, *142* (21), 9843−9849.
(45) Yadav, V.; Jaimes-Lizcano, Y. A.; Dewangan, N. K.; Park, N.; Li, T.-H.; Robertson, M. L.; Conrad, J. C. Tuning Bacterial Attachment and Detachment via the Thickness and Dispersity of a PH-Responsive Polymer Brush. *ACS Appl. Mater. Interfaces* **2017**, *9* (51), 44900−44910.
(46) Romio, M.; Grob, B.; Trachsel, L.; Mattarei, A.; Morgese, G.; Ramakrishna, S. N.; Niccolai, F.; Guazzelli, E.; Paradisi, C.; Martinelli, E.; Spencer, N. D.; Benetti, E. M. Dispersity within Brushes Plays a Major Role in Determining Their Interfacial Properties: The Case of Oligoxazoline-Based Graft Polymers. *J. Am. Chem. Soc.* **2021**, *143* (45), 19067−19077.
(47) Yadav, V.; Harkin, A. V.; Robertson, M. L.; Conrad, J. C. Hysteretic Memory in PH-Response of Water Contact Angle on Poly(Acrylic Acid) Brushes. *Soft Matter* **2016**, *12* (15), 3589−3599.
(48) Milner, S. T.; Witten, T. A.; Cates, M. E. Effects of Polydispersity in the End-Grafted Polymer Brush. *Macromolecules* **1989**, *22* (2), 853−861.
(49) de Vos, W. M.; Leermakers, F. A. M. Modeling the Structure of a Polydisperse Polymer Brush. *Polymer* **2009**, *50* (1), 305−316.
(50) Hyun, J.; Jang, H.; Kim, K.; Na, K.; Tak, T. Restriction of Biofouling in Membrane Filtration Using a Brush-like Polymer Containing Oligoethylene Glycol Side Chains. *J. Membr. Sci.* **2006**, *282* (1), 52−59.
(51) Ishak, N. F.; Hashim, N. A.; Othman, M. H. D.; Monash, P.; Zuki, F. M. Recent Progress in the Hydrophilic Modification of Alumina Membranes for Protein Separation and Purification. *Ceram. Int.* **2017**, *43* (1, Part B), 915−925.

https://doi.org/10.1021/jacsau.3c00081
JACS Au 2023, 3, 1284−1300

(52) Sun, W.; Liu, J.; Chu, H.; Dong, B. Pretreatment and Membrane Hydrophilic Modification to Reduce Membrane Fouling. *Membranes* **2013**, *3* (3), 226−241.
(53) Yang, F.; Huang, J.; Deng, L.; Zhang, Y.; Dang, G.; Shao, L. Hydrophilic Modification of Poly(Aryl Sulfone) Membrane Materials toward Highly-Efficient Environmental Remediation. *Front. Chem. Sci. Eng.* **2022**, *16* (5), 614−633.
(54) Goh, P. S.; Naim, R.; Rahbari-Sisakht, M.; Ismail, A. F. Modification of Membrane Hydrophobicity in Membrane Contactors for Environmental Remediation. *Sep. Purif. Technol.* **2019**, *227*, 115721.
(55) Ahmad, N. A.; Leo, C. P.; Ahmad, A. L.; Ramli, W. K. W. Membranes with Great Hydrophobicity: A Review on Preparation and Characterization. *Sep. Purif. Rev.* **2015**, *44* (2), 109−134.
(56) Kayser, L. V.; Lipomi, D. J. Stretchable Conductive Polymers and Composites Based on PEDOT and PEDOT:PSS. *Adv. Mater.* **2019**, *31* (10), 1806133.
(57) Yu, L.; Dean, K.; Li, L. Polymer Blends and Composites from Renewable Resources. *Prog. Polym. Sci.* **2006**, *31* (6), 576−602.
(58) Scaccabarozzi, A. D.; Stingelin, N. Semiconducting:Insulating Polymer Blends for Optoelectronic Applications—a Review of Recent Advances. *J. Mater. Chem. A* **2014**, *2* (28), 10818−10824.
(59) Lo, C.-Y.; Wu, Y.; Awuyah, E.; Meli, D.; Nguyen, D. M.; Wu, R.; Xu, B.; Strzalka, J.; Rivnay, J.; Martin, D. C.; Kayser, L. V. Influence of the Molecular Weight and Size Distribution of PSS on Mixed Ionic-Electronic Transport in PEDOT:PSS. *Polym. Chem.* **2022**, *13* (19), 2764−2775.
(60) Sun, K.; Zhang, S.; Li, P.; Xia, Y.; Zhang, X.; Du, D.; Isikgor, F. H.; Ouyang, J. Review on Application of PEDOTs and PEDOT:PSS in Energy Conversion and Storage Devices. *J. Mater. Sci. Mater. Electron.* **2015**, *26* (7), 4438−4462.
(61) Fan, X.; Nie, W.; Tsai, H.; Wang, N.; Huang, H.; Cheng, Y.; Wen, R.; Ma, L.; Yan, F.; Xia, Y. PEDOT:PSS for Flexible and Stretchable Electronics: Modifications, Strategies, and Applications. *Adv. Sci.* **2019**, *6* (19), 1900813.
(62) Groenendaal, L.; Jonas, F.; Freitag, D.; Pielartzik, H.; Reynolds, J. R. Poly(3,4-Ethylenedioxythiophene) and Its Derivatives: Past, Present, and Future. *Adv. Mater.* **2000**, *12* (7), 481−494.
(63) Paulsen, B. D.; Tybrandt, K.; Stavrinidou, E.; Rivnay, J. Organic Mixed Ionic−Electronic Conductors. *Nat. Mater.* **2020**, *19* (1), 13−26.
(64) Kim, D.; Kang, M.; Ha, H.; Hong, C. S.; Kim, M. Multiple Functional Groups in Metal−Organic Frameworks and Their Positional Regioisomerism. *Coord. Chem. Rev.* **2021**, *438*, 213892.
(65) Sheina, E. E.; Liu, J.; Iovu, M. C.; Laird, D. W.; McCullough, R. D. Chain Growth Mechanism for Regioregular Nickel-Initiated Cross-Coupling Polymerizations. *Macromolecules* **2004**, *37* (10), 3526−3528.
(66) Yokoyama, A.; Miyakoshi, R.; Yokozawa, T. Chain-Growth Polymerization for Poly(3-Hexylthiophene) with a Defined Molecular Weight and a Low Polydispersity. *Macromolecules* **2004**, *37* (4), 1169−1171.
(67) Childers, M. I.; Longo, J. M.; Van Zee, N. J.; LaPointe, A. M.; Coates, G. W. Stereoselective Epoxide Polymerization and Copolymerization. *Chem. Rev.* **2014**, *114* (16), 8129−8152.
(68) Xiao, S.; Zhang, Q.; You, W. Molecular Engineering of Conjugated Polymers for Solar Cells: An Updated Report. *Adv. Mater.* **2017**, *29* (20), 1601391.
(69) Li, G.; Chang, W.-H.; Yang, Y. Low-Bandgap Conjugated Polymers Enabling Solution-Processable Tandem Solar Cells. *Nat. Rev. Mater.* **2017**, *2* (8), 1−13.
(70) Marrocchi, A.; Lanari, D.; Facchetti, A.; Vaccaro, L. Poly(3-Hexylthiophene): Synthetic Methodologies and Properties in Bulk Heterojunction Solar Cells. *Energy Environ. Sci.* **2012**, *5* (9), 8457−8474.
(71) Laquai, F.; Andrienko, D.; Mauer, R.; Blom, P. W. M. Charge Carrier Transport and Photogeneration in P3HT:PCBM Photovoltaic Blends. *Macromol. Rapid Commun.* **2015**, *36* (11), 1001−1025.
(72) Kim, Y.; Cook, S.; Tuladhar, S. M.; Choulis, S. A.; Nelson, J.; Durrant, J. R.; Bradley, D. D. C.; Giles, M.; McCulloch, I.; Ha, C.-S.; Ree, M. A Strong Regioregularity Effect in Self-Organizing Conjugated Polymer Films and High-Efficiency Polythiophene:Fullerene Solar Cells. *Nat. Mater.* **2006**, *5* (3), 197−203.
(73) Chu, P.-H.; Wang, G.; Fu, B.; Choi, D.; Park, J. O.; Srinivasarao, M.; Reichmanis, E. Synergistic Effect of Regioregular and Regiorandom Poly(3-Hexylthiophene) Blends for High Performance Flexible Organic Field Effect Transistors. *Adv. Electron. Mater.* **2016**, *2* (2), 1500384.
(74) Park, H.; Ma, B. S.; Kim, J.-S.; Kim, Y.; Kim, H. J.; Kim, D.; Yun, H.; Han, J.; Kim, F. S.; Kim, T.-S.; Kim, B. J. Regioregular-Block-Regiorandom Poly(3-Hexylthiophene) Copolymers for Mechanically Robust and High-Performance Thin-Film Transistors. *Macromolecules* **2019**, *52* (20), 7721−7730.
(75) Zhang, Z.-G.; Wang, J. Structures and Properties of Conjugated Donor−Acceptor Copolymers for Solar Cell Applications. *J. Mater. Chem.* **2012**, *22* (10), 4178−4187.
(76) Yuen, J. D.; Wudl, F. Strong Acceptors in Donor−Acceptor Polymers for High Performance Thin Film Transistors. *Energy Environ. Sci.* **2013**, *6* (2), 392−406.
(77) Steyrleuthner, R.; Di Pietro, R.; Collins, B. A.; Polzer, F.; Himmelberger, S.; Schubert, M.; Chen, Z.; Zhang, S.; Salleo, A.; Ade, H.; Facchetti, A.; Neher, D. The Role of Regioregularity, Crystallinity, and Chain Orientation on Electron Transport in a High-Mobility n-Type Copolymer. *J. Am. Chem. Soc.* **2014**, *136* (11), 4245−4256.
(78) Gross, Y. M.; Trefz, D.; Tkachov, R.; Untilova, V.; Brinkmann, M.; Schulz, G. L.; Ludwigs, S. Tuning Aggregation by Regioregularity for High-Performance n-Type P(NDI2OD-T2) Donor−Acceptor Copolymers. *Macromolecules* **2017**, *50* (14), 5353−5366.
(79) Treat, N. D.; Shuttle, C. G.; Toney, M. F.; Hawker, C. J.; Chabinyc, M. L. In Situ Measurement of Power Conversion Efficiency and Molecular Ordering during Thermal Annealing in P3HT:PCBM Bulk Heterojunction Solar Cells. *J. Mater. Chem.* **2011**, *21* (39), 15224−15231.
(80) McKeown, N. B.; Budd, P. M. Polymers of Intrinsic Microporosity (PIMs): Organic Materials for Membrane Separations, Heterogeneous Catalysis and Hydrogen Storage. *Chem. Soc. Rev.* **2006**, *35* (8), 675−683.
(81) Hu, X.; Miao, J.; Pang, Y.; Zhao, J.; Lu, Y.; Guo, H.; Wang, Z.; Yan, J. Synthesis, Microstructures, and Gas Separation Performance of Norbornyl Bis-Benzocyclobutene-Tröger's Base Polymers Derived from Pure Regioisomers. *Polym. Chem.* **2022**, *13* (19), 2842−2849.
(82) Short, R.; Carta, M.; Bezzu, C. G.; Fritsch, D.; Kariuki, B. M.; McKeown, N. B. Hexaphenylbenzene-Based Polymers of Intrinsic Microporosity. *Chem. Commun.* **2011**, *47* (24), 6822−6824.
(83) Zhu, Z.; Zhu, J.; Li, J.; Ma, X. Enhanced Gas Separation Properties of Tröger's Base Polymer Membranes Derived from Pure Triptycene Diamine Regioisomers. *Macromolecules* **2020**, *53* (5), 1573−1584.
(84) Liu, S.; Jin, Z.; Teo, Y. C.; Xia, Y. Efficient Synthesis of Rigid Ladder Polymers via Palladium Catalyzed Annulation. *J. Am. Chem. Soc.* **2014**, *136* (50), 17434−17437.
(85) Ma, X.; Lai, H. W. H.; Wang, Y.; Alhazmi, A.; Xia, Y.; Pinnau, I. Facile Synthesis and Study of Microporous Catalytic Arene-Norbornene Annulation−Tröger's Base Ladder Polymers for Membrane Air Separation. *ACS Macro Lett.* **2020**, *9* (5), 680−685.
(86) Rajalingam, P.; Radhakrishxan, G. Polyacrylonitrile Precursor for Carbon Fibers. *J. Macromol. Sci. Part C* **1991**, *31* (2−3), 301−310.
(87) Coates, G. W. Precise Control of Polyolefin Stereochemistry Using Single-Site Metal Catalysts. *Chem. Rev.* **2000**, *100* (4), 1223−1252.
(88) Corradini, P.; Guerra, G.; Cavallo, L. Do New Century Catalysts Unravel the Mechanism of Stereocontrol of Old Ziegler−Natta Catalysts? *Acc. Chem. Res.* **2004**, *37* (4), 231−241.
(89) Busico, V.; Cipullo, R. Microstructure of Polypropylene. *Prog. Polym. Sci.* **2001**, *26* (3), 443−533.
(90) Hackler, R. A.; Lamb, J. V.; Peczak, I. L.; Kennedy, R. M.; Kanbur, U.; LaPointe, A. M.; Poeppelmeier, K. R.; Sadow, A. D.;

https://doi.org/10.1021/jacsau.3c00081
JACS Au 2023, 3, 1284−1300

Delferro, M. Effect of Macro- and Microstructures on Catalytic Hydrogenolysis of Polyolefins. *Macromolecules* **2022**, *55*, 6801.
(91) Pinijmontree, T.; Vao-soongnern, V. Dynamics of Polypropylene Chains in Their Binary Blends of Different Stereochemical Sequences Studied by Monte Carlo Simulations. *Chin. J. Polym. Sci.* **2014**, *32* (5), 640−649.
(92) Grignard, B.; Gennen, S.; Jerome, C.; Kleij, A. W.; Detrembleur, C. Advances in the Use of CO 2 as a Renewable Feedstock for the Synthesis of Polymers. *Chem. Soc. Rev.* **2019**, *48* (16), 4466−4514.
(93) Mohanty, A. K.; Wu, F.; Mincheva, R.; Hakkarainen, M.; Raquez, J.-M.; Mielewski, D. F.; Narayan, R.; Netravali, A. N.; Misra, M. Sustainable Polymers. *Nat. Rev. Methods Primer* **2022**, *2* (1), 1−27.
(94) Hatti-Kaul, R.; Nilsson, L. J.; Zhang, B.; Rehnberg, N.; Lundmark, S. Designing Biobased Recyclable Polymers for Plastics. *Trends Biotechnol.* **2020**, *38* (1), 50−67.
(95) Bai, H.; Deng, S.; Bai, D.; Zhang, Q.; Fu, Q. Recent Advances in Processing of Stereocomplex-Type Polylactide. *Macromol. Rapid Commun.* **2017**, *38* (23), 1700454.
(96) Stanford, M. J.; Dove, A. P. Stereocontrolled Ring-Opening Polymerisation of Lactide. *Chem. Soc. Rev.* **2010**, *39* (2), 486−494.
(97) Becker, J. M.; Pounder, R. J.; Dove, A. P. Synthesis of Poly(Lactide)s with Modified Thermal and Mechanical Properties. *Macromol. Rapid Commun.* **2010**, *31* (22), 1923−1937.
(98) Chile, L.-E.; Mehrkhodavandi, P.; Hatzikiriakos, S. G. A Comparison of the Rheological and Mechanical Properties of Isotactic, Syndiotactic, and Heterotactic Poly(Lactide. *Macromolecules* **2016**, *49* (3), 909−919.
(99) Tang, X.; Chen, E. Y.-X. Chemical Synthesis of Perfectly Isotactic and High Melting Bacterial Poly(3-Hydroxybutyrate) from Bio-Sourced Racemic Cyclic Diolide. *Nat. Commun.* **2018**, *9* (1), 2345.
(100) Ajellal, N.; Bouyahyi, M.; Amgoune, A.; Thomas, C. M.; Bondon, A.; Pillin, I.; Grohens, Y.; Carpentier, J.-F. Syndiotactic-Enriched Poly(3-Hydroxybutyrate)s via Stereoselective Ring-Opening Polymerization of Racemic β-Butyrolactone with Discrete Yttrium Catalysts. *Macromolecules* **2009**, *42* (4), 987−993.
(101) Bloembergen, S.; Holden, D. A.; Bluhm, T. L.; Hamer, G. K.; Marchessault, R. H. Stereoregularity in Synthetic β-Hydroxybutyrate and β-Hydroxyvalerate Homopolyesters. *Macromolecules* **1989**, *22* (4), 1656−1663.
(102) Kramer, J. W.; Treitler, D. S.; Dunn, E. W.; Castro, P. M.; Roisnel, T.; Thomas, C. M.; Coates, G. W. Polymerization of Enantiopure Monomers Using Syndiospecific Catalysts: A New Approach To Sequence Control in Polymer Synthesis. *J. Am. Chem. Soc.* **2009**, *131* (44), 16042−16044.
(103) Pearce, R.; Jesudason, J.; Orts, W.; Marchessault, R. H.; Bloembergen, S. Blends of Bacterial and Synthetic Poly(β-Hydroxybutyrate): Effect of Tacticity on Melting Behaviour. *Polymer* **1992**, *33* (21), 4647−4649.
(104) Pearce, R.; Marchessault, R. H. Multiple Melting in Blends of Isotactic and Atactic Poly(β-Hydroxybutyrate. *Polymer* **1994**, *35* (18), 3990−3997.
(105) Elsawy, M. A.; Kim, K.-H.; Park, J.-W.; Deep, A. Hydrolytic Degradation of Polylactic Acid (PLA) and Its Composites. *Renew. Sustain. Energy Rev.* **2017**, *79*, 1346−1352.
(106) Stubbs, C. J.; Worch, J. C.; Prydderch, H.; Wang, Z.; Mathers, R. T.; Dobrynin, A. V.; Becker, M. L.; Dove, A. P. Sugar-Based Polymers with Stereochemistry-Dependent Degradability and Mechanical Properties. *J. Am. Chem. Soc.* **2022**, *144* (3), 1243−1250.
(107) Khalfa, A. L.; Becker, M. L.; Dove, A. P. Stereochemistry-Controlled Mechanical Properties and Degradation in 3D-Printable Photosets. *J. Am. Chem. Soc.* **2021**, *143* (42), 17510−17516.
(108) Short, J. N.; Kraus, G.; Zelinski, R. P.; Naylor, F. E. Polybutadienes of Controlled Cis, Trans and Vinyl Structures. *Rubber Chem. Technol.* **1959**, *32* (2), 614−627.
(109) Feng, Q.-K.; Zhong, S.-L.; Pei, J.-Y.; Zhao, Y.; Zhang, D.-L.; Liu, D.-F.; Zhang, Y.-X.; Dang, Z.-M. Recent Progress and Future Prospects on All-Organic Polymer Dielectrics for Energy Storage Capacitors. *Chem. Rev.* **2022**, *122* (3), 3820−3878.
(110) Rabuffi, M.; Picci, G. Status Quo and Future Prospects for Metallized Polypropylene Energy Storage Capacitors. *IEEE Trans. Plasma Sci.* **2002**, *30* (5), 1939−1942.
(111) Nash, J. L. Biaxially Oriented Polypropylene Film in Power Capacitors. *Polym. Eng. Sci.* **1988**, *28* (13), 862−870.
(112) Artbauer, J. Electric Strength of Polymers. *J. Phys. Appl. Phys.* **1996**, *29* (2), 446.
(113) Park, J. H.; Hwang, D. K.; Lee, J.; Im, S.; Kim, E. Studies on Poly(Methyl Methacrylate) Dielectric Layer for Field Effect Transistor: Influence of Polymer Tacticity. *Thin Solid Films* **2007**, *515* (7), 4041−4044.
(114) Wang, Y.; Nakamura, R.; Suga, T.; Li, S.; Ohki, Y.; Nishide, H.; Oyaizu, K. Facile Synthesis of Isotactic Polyacrylonitrile via Template Polymerization in Interlayer Space for Dielectric Energy Storage. *ACS Appl. Polym. Mater.* **2020**, *2* (2), 775−781.
(115) Wong, M. Y. Recent Advances in Polymer Organic Light-Emitting Diodes (PLED) Using Non-Conjugated Polymers as the Emitting Layer and Contrasting Them with Conjugated Counterparts. *J. Electron. Mater.* **2017**, *46* (11), 6246−6281.
(116) Gallego, J.; Pérez-Foullerat, D.; Mendicuti, F.; Mattice, W. L. Configurations Conducive to the Formation of Intramolecular Excimers in Poly(N-Vinyl Carbazole) and Its Copolymers. *J. Polym. Sci., Part B: Polym. Phys.* **2001**, *39* (12), 1272−1281.
(117) Karali, A.; Dais, P.; Mikros, E.; Heatley, F. Conformational Analysis of Poly(N-Vinylcarbazole) by NMR Spectroscopy and Molecular Modeling. *Macromolecules* **2001**, *34* (16), 5547−5554.
(118) Samal, S.; Schmitt, A.; Thompson, B. C. Contrasting the Charge Carrier Mobility of Isotactic, Syndiotactic, and Atactic Poly((N-Carbazolylethylthio)Propyl Methacrylate. *ACS Macro Lett.* **2021**, *10* (12), 1493−1500.
(119) Samal, S.; Thompson, B. C. Converging the Hole Mobility of Poly(2-N-Carbazoylethyl Acrylate) with Conjugated Polymers by Tuning Isotacticity. *ACS Macro Lett.* **2018**, *7* (10), 1161−1167.
(120) Schmitt, A.; Kazerouni, N.; Castillo, G. E.; Thompson, B. C. Synthesis of Block Copolymers Containing Stereoregular Pendant Electroactive Blocks. *ACS Macro Lett.* **2023**, *12*, 159−164.
(121) Uryu, T.; Ohkawa, H.; Oshima, R. Synthesis and High Hole Mobility of Isotactic Poly(2-N-Carbazolylethyl Acrylate. *Macromolecules* **1987**, *20* (4), 712−716.
(122) Lutz, J.-F. Defining the Field of Sequence-Controlled Polymers. *Macromol. Rapid Commun.* **2017**, *38* (24), 1700582.
(123) Dong, R.; Liu, R.; Gaffney, P. R. J.; Schaepertoens, M.; Marchetti, P.; Williams, C. M.; Chen, R.; Livingston, A. G. Sequence-Defined Multifunctional Polyethers via Liquid-Phase Synthesis with Molecular Sieving. *Nat. Chem.* **2019**, *11* (2), 136−145.
(124) Holloway, J. O.; Wetzel, K. S.; Martens, S.; Du Prez, F. E.; Meier, M. A. R. Direct Comparison of Solution and Solid Phase Synthesis of Sequence-Defined Macromolecules. *Polym. Chem.* **2019**, *10* (28), 3859−3867.
(125) Xu, C.; He, C.; Li, N.; Yang, S.; Du, Y.; Matyjaszewski, K.; Pan, X. Regio- and Sequence-Controlled Conjugated Topological Oligomers and Polymers via Boronate-Tag Assisted Solution-Phase Strategy. *Nat. Commun.* **2021**, *12* (1), 5853.
(126) Chen, W.; Schuster, G. B. Precise Sequence Control in Linear and Cyclic Copolymers of 2,5-Bis(2-Thienyl)Pyrrole and Aniline by DNA-Programmed Assembly. *J. Am. Chem. Soc.* **2013**, *135* (11), 4438−4449.
(127) Milnes, P. J.; McKee, M. L.; Bath, J.; Song, L.; Stulz, E.; Turberfield, A. J.; O'Reilly, R. K. Sequence-Specific Synthesis of Macromolecules Using DNA-Templated Chemistry. *Chem. Commun.* **2012**, *48* (45), 5614−5616.
(128) McKee, M. L.; Milnes, P. J.; Bath, J.; Stulz, E.; Turberfield, A. J.; O'Reilly, R. K. Multistep DNA-Templated Reactions for the Synthesis of Functional Sequence Controlled Oligomers. *Angew. Chem.* **2010**, *122* (43), 8120−8123.
(129) ten Brummelhuis, N. Controlling Monomer-Sequence Using Supramolecular Templates. *Polym. Chem.* **2015**, *6* (5), 654−667.

https://doi.org/10.1021/jacsau.3c00081
JACS Au 2023, 3, 1284−1300

(130) Ida, S.; Ouchi, M.; Sawamoto, M. Template-Assisted Selective Radical Addition toward Sequence-Regulated Polymerization: Lariat Capture of Target Monomer by Template Initiator. *J. Am. Chem. Soc.* **2010**, *132* (42), 14748−14750.
(131) Meng, W.; Muscat, R. A.; McKee, M. L.; Milnes, P. J.; El-Sagheer, A. H.; Bath, J.; Davis, B. G.; Brown, T.; O'Reilly, R. K.; Turberfield, A. J. An Autonomous Molecular Assembler for Programmable Chemical Synthesis. *Nat. Chem.* **2016**, *8* (6), 542−548.
(132) Xu, J.; Fu, C.; Shanmugam, S.; Hawker, C. J.; Moad, G.; Boyer, C. Synthesis of Discrete Oligomers by Sequential PET-RAFT Single-Unit Monomer Insertion. *Angew. Chem., Int. Ed.* **2017**, *56* (29), 8376−8383.
(133) Shanmugam, S.; Cuthbert, J.; Kowalewski, T.; Boyer, C.; Matyjaszewski, K. Catalyst-Free Selective Photoactivation of RAFT Polymerization: A Facile Route for Preparation of Comblike and Bottlebrush Polymers. *Macromolecules* **2018**, *51* (19), 7776−7784.
(134) Barnes, J. C.; Ehrlich, D. J. C.; Gao, A. X.; Leibfarth, F. A.; Jiang, Y.; Zhou, E.; Jamison, T. F.; Johnson, J. A. Iterative Exponential Growth of Stereo- and Sequence-Controlled Polymers. *Nat. Chem.* **2015**, *7* (10), 810−815.
(135) Leibfarth, F. A.; Johnson, J. A.; Jamison, T. F. Scalable Synthesis of Sequence-Defined, Unimolecular Macromolecules by Flow-IEG. *Proc. Natl. Acad. Sci. U. S. A.* **2015**, *112* (34), 10617−10622.
(136) Steinkoenig, J.; Aksakal, R.; Du Prez, F. Molecular Access to Multi-Dimensionally Encoded Information. *Eur. Polym. J.* **2019**, *120*, 109260.
(137) Aksakal, R.; Mertens, C.; Soete, M.; Badi, N.; Du Prez, F. Applications of Discrete Synthetic Macromolecules in Life and Materials Science: Recent and Future Trends. *Adv. Sci.* **2021**, *8* (6), 2004038.
(138) Karamessini, D.; Poyer, S.; Charles, L.; Lutz, J.-F. 2D Sequence-Coded Oligourethane Barcodes for Plastic Materials Labeling. *Macromol. Rapid Commun.* **2017**, *38* (24), 1700426.
(139) Martens, S.; Landuyt, A.; Espeel, P.; Devreese, B.; Dawyndt, P.; Du Prez, F. Multifunctional Sequence-Defined Macromolecules for Chemical Data Storage. *Nat. Commun.* **2018**, *9* (1), 4451.
(140) Samokhvalova, S.; Lutz, J.-F. Macromolecular Information Transfer. *Angew. Chem., Int. Ed.* **2023**, e202300014.
(141) Sun, Y.; Tan, R.; Ma, Z.; Gan, Z.; Li, G.; Zhou, D.; Shao, Y.; Zhang, W.-B.; Zhang, R.; Dong, X.-H. Discrete Block Copolymers with Diverse Architectures: Resolving Complex Spherical Phases with One Monomer Resolution. *ACS Cent. Sci.* **2020**, *6* (8), 1386−1393.
(142) Rosales, A. M.; Segalman, R. A.; Zuckermann, R. N. Polypeptoids: A Model System to Study the Effect of Monomer Sequence on Polymer Properties and Self-Assembly. *Soft Matter* **2013**, *9* (35), 8400−8414.
(143) Li, Z.; Cai, B.; Yang, W.; Chen, C.-L. Hierarchical Nanomaterials Assembled from Peptoids and Other Sequence-Defined Synthetic Polymers. *Chem. Rev.* **2021**, *121* (22), 14031−14087.
(144) Lau, K. H. A.; Sileika, T. S.; Park, S. H.; Sousa, A. M. L.; Burch, P.; Szleifer, I.; Messersmith, P. B. Molecular Design of Antifouling Polymer Brushes Using Sequence-Specific Peptoids. *Adv. Mater. Interfaces* **2015**, *2* (1), 1400225.
(145) van Zoelen, W.; Buss, H. G.; Ellebracht, N. C.; Lynd, N. A.; Fischer, D. A.; Finlay, J.; Hill, S.; Callow, M. E.; Callow, J. A.; Kramer, E. J.; Zuckermann, R. N.; Segalman, R. A. Sequence of Hydrophobic and Hydrophilic Residues in Amphiphilic Polymer Coatings Affects Surface Structure and Marine Antifouling/Fouling Release Properties. *ACS Macro Lett.* **2014**, *3* (4), 364−368.
(146) Bates, F. S.; Hillmyer, M. A.; Lodge, T. P.; Bates, C. M.; Delaney, K. T.; Fredrickson, G. H. Multiblock Polymers: Panacea or Pandora's Box? *Science* **2012**, *336* (6080), 434−440.
(147) Eagan, J. M.; Xu, J.; Di Girolamo, R.; Thurber, C. M.; Macosko, C. W.; LaPointe, A. M.; Bates, F. S.; Coates, G. W. Combining Polyethylene and Polypropylene: Enhanced Performance with PE/IPP Multiblock Polymers. *Science* **2017**, *355* (6327), 814−816.
(148) Xu, J.; Eagan, J. M.; Kim, S.-S.; Pan, S.; Lee, B.; Klimovica, K.; Jin, K.; Lin, T.-W.; Howard, M. J.; Ellison, C. J.; LaPointe, A. M.; Coates, G. W.; Bates, F. S. Compatibilization of Isotactic Polypropylene (IPP) and High-Density Polyethylene (HDPE) with IPP−PE Multiblock Copolymers. *Macromolecules* **2018**, *51* (21), 8585−8596.
(149) Cooper, C. B.; Bao, Z. Using Periodic Dynamic Polymers to Form Supramolecular Nanostructures. *Acc. Mater. Res.* **2022**, *3* (9), 948−959.
(150) Park, J.; Winey, K. I. Double Gyroid Morphologies in Precise Ion-Containing Multiblock Copolymers Synthesized via Step-Growth Polymerization. *JACS Au* **2022**, *2*, 1769.
(151) Baughman, T. W.; Chan, C. D.; Winey, K. I.; Wagener, K. B. Synthesis and Morphology of Well-Defined Poly(Ethylene-Co-Acrylic Acid) Copolymers. *Macromolecules* **2007**, *40* (18), 6564−6571.
(152) Trigg, E. B.; Gaines, T. W.; Maréchal, M.; Moed, D. E.; Rannou, P.; Wagener, K. B.; Stevens, M. J.; Winey, K. I. Self-Assembled Highly Ordered Acid Layers in Precisely Sulfonated Polyethylene Produce Efficient Proton Transport. *Nat. Mater.* **2018**, *17* (8), 725−731.
(153) Yan, L.; Rank, C.; Mecking, S.; Winey, K. I. Gyroid and Other Ordered Morphologies in Single-Ion Conducting Polymers and Their Impact on Ion Conductivity. *J. Am. Chem. Soc.* **2020**, *142* (2), 857−866.
(154) Voit, B. I.; Lederer, A. Hyperbranched and Highly Branched Polymer Architectures—Synthetic Strategies and Major Characterization Aspects. *Chem. Rev.* **2009**, *109* (11), 5924−5973.
(155) Gao, C.; Yan, D. Hyperbranched Polymers: From Synthesis to Applications. *Prog. Polym. Sci.* **2004**, *29* (3), 183−275.
(156) Potemkin, I. I.; Palyulin, V. V. Comblike Macromolecules. *Polym. Sci. Ser. A* **2009**, *51* (2), 123−149.
(157) Sheiko, S. S.; Sumerlin, B. S.; Matyjaszewski, K. Cylindrical Molecular Brushes: Synthesis, Characterization, and Properties. *Prog. Polym. Sci.* **2008**, *33* (7), 759−785.
(158) Kim, K. H.; Nam, J.; Choi, J.; Seo, M.; Bang, J. From Macromonomers to Bottlebrush Copolymers with Sequence Control: Synthesis, Properties, and Applications. *Polym. Chem.* **2022**, *13* (16), 2224−2261.
(159) Xie, G.; Martinez, M. R.; Olszewski, M.; Sheiko, S. S.; Matyjaszewski, K. Molecular Bottlebrushes as Novel Materials. *Biomacromolecules* **2019**, *20* (1), 27−54.
(160) Rzayev, J. Molecular Bottlebrushes: New Opportunities in Nanomaterials Fabrication. *ACS Macro Lett.* **2012**, *1* (9), 1146−1149.
(161) Verduzco, R.; Li, X.; Pesek, S. L.; Stein, G. E. Structure, Function, Self-Assembly, and Applications of Bottlebrush Copolymers. *Chem. Soc. Rev.* **2015**, *44* (8), 2405−2420.
(162) Pelras, T.; Mahon, C. S.; Müllner, M. Synthesis and Applications of Compartmentalised Molecular Polymer Brushes. *Angew. Chem., Int. Ed.* **2018**, *57* (24), 6982−6994.
(163) Feng, C.; Li, Y.; Yang, D.; Hu, J.; Zhang, X.; Huang, X. Well-Defined Graft Copolymers: From Controlled Synthesis to Multipurpose Applications. *Chem. Soc. Rev.* **2011**, *40* (3), 1282−1295.
(164) Ren, J. M.; McKenzie, T. G.; Fu, Q.; Wong, E. H. H.; Xu, J.; An, Z.; Shanmugam, S.; Davis, T. P.; Boyer, C.; Qiao, G. G. Star Polymers. *Chem. Rev.* **2016**, *116* (12), 6743−6836.
(165) Cao, M.; Zhong, M. Chain-Growth Branching Radical Polymerization: An Inibramer Strategy. *Polym. Int.* **2022**, *71* (5), 501−507.
(166) Kapil, K.; Szczepaniak, G.; Martinez, M. R.; Murata, H.; Jazani, A. M.; Jeong, J.; Das, S. R.; Matyjaszewski, K. Visible-Light-Mediated Controlled Radical Branching Polymerization in Water. *Angew. Chem., Int. Ed.* **2023**, *62* (10), e202217658.
(167) Li, F.; Cao, M.; Feng, Y.; Liang, R.; Fu, X.; Zhong, M. Site-Specifically Initiated Controlled/Living Branching Radical Polymerization: A Synthetic Route toward Hierarchically Branched Architectures. *J. Am. Chem. Soc.* **2019**, *141* (2), 794−799.

https://doi.org/10.1021/jacsau.3c00081
JACS Au 2023, 3, 1284−1300

(168) Zhao, Y.; Ma, M.; Lin, X.; Chen, M. Photoorganocatalyzed Divergent Reversible-Deactivation Radical Polymerization towards Linear and Branched Fluoropolymers. *Angew. Chem., Int. Ed.* **2020**, *59* (48), 21470−21474.
(169) Cao, M.; Liu, Y.; Zhang, X.; Li, F.; Zhong, M. Expanding the Toolbox of Controlled/Living Branching Radical Polymerization through Simulation-Informed Reaction Design. *Chem.* **2022**, *8* (5), 1460−1475.
(170) Lu, Y.; Nemoto, T.; Tosaka, M.; Yamago, S. Synthesis of Structurally Controlled Hyperbranched Polymers Using a Monomer Having Hierarchical Reactivity. *Nat. Commun.* **2017**, *8* (1), 1863.
(171) Shi, Y.; Graff, R. W.; Cao, X.; Wang, X.; Gao, H. Chain-Growth Click Polymerization of AB2Monomers for the Formation of Hyperbranched Polymers with Low Polydispersities in a One-Pot Process. *Angew. Chem.* **2015**, *127* (26), 7741−7745.
(172) Zhang, Y.; Cui, C.; Sun, Y.; Zhang, X.; Yang, R.; Yang, J.; Xie, F.; Liu, W. A Hyperbranched Polymer-Based Water-Resistant Adhesive: Durable Underwater Adhesion and Primer for Anchoring Anti-Fouling Hydrogel Coating. *Sci. China Technol. Sci.* **2022**, *65* (1), 201−213.
(173) Li, X.; Cai, T.; Chung, T.-S. Anti-Fouling Behavior of Hyperbranched Polyglycerol-Grafted Poly(Ether Sulfone) Hollow Fiber Membranes for Osmotic Power Generation. *Environ. Sci. Technol.* **2014**, *48* (16), 9898−9907.
(174) Ai, X.; Mei, L.; Ma, C.; Zhang, G. Degradable Hyperbranched Polymer with Fouling Resistance for Antifouling Coatings. *Prog. Org. Coat.* **2021**, *153*, 106141.
(175) Chen, P.-R.; Wang, T.-C.; Chen, S.-T.; Chen, H.-Y.; Tsai, W.-B. Development of Antifouling Hyperbranched Polyglycerol Layers on Hydroxyl Poly-p-Xylylene Coatings. *Langmuir* **2017**, *33* (51), 14657−14662.
(176) Reichelt, S.; Eichhorn, K.-J.; Aulich, D.; Hinrichs, K.; Jain, N.; Appelhans, D.; Voit, B. Functionalization of Solid Surfaces with Hyperbranched Polyesters to Control Protein Adsorption. *Colloids Surf. B Biointerfaces* **2009**, *69* (2), 169−177.
(177) Gudipati, C. S.; Greenlief, C. M.; Johnson, J. A.; Prayongpan, P.; Wooley, K. L. Hyperbranched Fluoropolymer and Linear Poly(Ethylene Glycol) Based Amphiphilic Crosslinked Networks as Efficient Antifouling Coatings: An Insight into the Surface Compositions, Topographies, and Morphologies. *J. Polym. Sci. Part Polym. Chem.* **2004**, *42* (24), 6193−6208.
(178) Dai, G.; Ai, X.; Mei, L.; Ma, C.; Zhang, G. Kill−Resist−Renew Trinity: Hyperbranched Polymer with Self-Regenerating Attack and Defense for Antifouling Coatings. *ACS Appl. Mater. Interfaces* **2021**, *13* (11), 13735−13743.
(179) Imbesi, P. M.; Fidge, C.; Raymond, J. E.; Cauët, S. I.; Wooley, K. L. Model Diels−Alder Studies for the Creation of Amphiphilic Cross-Linked Networks as Healable, Antibiofouling Coatings. *ACS Macro Lett.* **2012**, *1* (4), 473−477.
(180) Imbesi, P. M.; Gohad, N. V.; Eller, M. J.; Orihuela, B.; Rittschof, D.; Schweikert, E. A.; Mount, A. S.; Wooley, K. L. Noradrenaline-Functionalized Hyperbranched Fluoropolymer−Poly(Ethylene Glycol) Cross-Linked Networks As Dual-Mode, Anti-Biofouling Coatings. *ACS Nano* **2012**, *6* (2), 1503−1512.
(181) Cai, T.; Yang, W. J.; Neoh, K.-G.; Kang, E.-T. Poly(Vinylidene Fluoride) Membranes with Hyperbranched Antifouling and Antibacterial Polymer Brushes. *Ind. Eng. Chem. Res.* **2012**, *51* (49), 15962−15973.
(182) Mei, L.; Ai, X.; Ma, C.; Zhang, G. Surface-Fragmenting Hyperbranched Copolymers with Hydrolysis-Generating Zwitterions for Antifouling Coatings. *J. Mater. Chem. B* **2020**, *8* (25), 5434−5440.
(183) Moore, E.; Delalat, B.; Vasani, R.; McPhee, G.; Thissen, H.; Voelcker, N. H. Surface-Initiated Hyperbranched Polyglycerol as an Ultralow-Fouling Coating on Glass, Silicon, and Porous Silicon Substrates. *ACS Appl. Mater. Interfaces* **2014**, *6* (17), 15243−15252.
(184) Wang, X.; Wang, Z.; Wang, Z.; Cao, Y.; Meng, J. Tethering of Hyperbranched Polyols Using PEI as a Building Block to Synthesize Antifouling PVDF Membranes. *Appl. Surf. Sci.* **2017**, *419*, 546−556.
(185) Ai, X.; Pan, J.; Xie, Q.; Ma, C.; Zhang, G. UV-Curable Hyperbranched Poly(Ester-Co-Vinyl) by Radical Ring-Opening Copolymerization for Antifouling Coatings. *Polym. Chem.* **2021**, *12* (31), 4524−4531.
(186) Zheng, X.; Zhang, C.; Bai, L.; Liu, S.; Tan, L.; Wang, Y. Antifouling Property of Monothiol-Terminated Bottle-Brush Poly(Methylacrylic Acid)-Graft-Poly(2-Methyl-2-Oxazoline) Copolymer on Gold Surfaces. *J. Mater. Chem. B* **2015**, *3* (9), 1921−1930.
(187) Banquy, X.; Burdyńska, J.; Lee, D. W.; Matyjaszewski, K.; Israelachvili, J. Bioinspired Bottle-Brush Polymer Exhibits Low Friction and Amontons-like Behavior. *J. Am. Chem. Soc.* **2014**, *136* (17), 6199−6202.
(188) Xia, Y.; Adibnia, V.; Huang, R.; Murschel, F.; Faivre, J.; Xie, G.; Olszewski, M.; De Crescenzo, G.; Qi, W.; He, Z.; Su, R.; Matyjaszewski, K.; Banquy, X. Biomimetic Bottlebrush Polymer Coatings for Fabrication of Ultralow Fouling Surfaces. *Angew. Chem., Int. Ed.* **2019**, *58* (5), 1308−1314.
(189) Morgese, G.; Gombert, Y.; Ramakrishna, S. N.; Benetti, E. M. Mixing Poly(Ethylene Glycol) and Poly(2-Alkyl-2-Oxazoline)s Enhances Hydration and Viscoelasticity of Polymer Brushes and Determines Their Nanotribological and Antifouling Properties. *ACS Appl. Mater. Interfaces* **2018**, *10* (48), 41839−41848.
(190) Gao, Q.; Yu, M.; Su, Y.; Xie, M.; Zhao, X.; Li, P.; Ma, P. X. Rationally Designed Dual Functional Block Copolymers for Bottlebrush-like Coatings: In Vitro and in Vivo Antimicrobial, Antibiofilm, and Antifouling Properties. *Acta Biomater.* **2017**, *51*, 112−124.
(191) Kim, D.-G.; Kang, H.; Han, S.; Lee, J.-C. The Increase of Antifouling Properties of Ultrafiltration Membrane Coated by Star-Shaped Polymers. *J. Mater. Chem.* **2012**, *22* (17), 8654−8661.
(192) Jeon, S.; Shin, S. S.; Park, C. H.; Lee, J.-H. Star Polymer-Mediated in-Situ Synthesis of Silver-Incorporated Reverse Osmosis Membranes with Excellent and Durable Biofouling Resistance. *J. Membr. Sci.* **2021**, *639*, 119778.
(193) Bargathulla, I.; Manivannan, N.; Gopinath, A.; Mathivanan, N.; Nasar, A. S. High Density Star Poly HEMA Containing Bis-Indole Rich Dendrimer Inner Core for Integrated Anti-Fouling and Anti-Bacterial Coating Applications. *Eur. Polym. J.* **2022**, *170*, 111170.
(194) Diep, J.; Tek, A.; Thompson, L.; Frommer, J.; Wang, R.; Piunova, V.; Sly, J.; La, Y.-H. Layer-by-Layer Assembled Core−Shell Star Block Copolymers for Fouling Resistant Water Purification Membranes. *Polymer* **2016**, *103*, 468−477.
(195) Soltannia, B.; Islam, M. A.; Cho, J.-Y.; Mohammadtabar, F.; Wang, R.; Piunova, V. A.; Almansoori, Z.; Rastgar, M.; Myles, A. J.; La, Y.-H.; Sadrzadeh, M. Thermally Stable Core-Shell Star-Shaped Block Copolymers for Antifouling Enhancement of Water Purification Membranes. *J. Membr. Sci.* **2020**, *598*, 117686.
(196) Kim, D.-G.; Kang, H.; Choi, Y.-S.; Han, S.; Lee, J.-C. Photo-Cross-Linkable Star-Shaped Polymers with Poly(Ethylene Glycol) and Renewable Cardanol Side Groups: Synthesis, Characterization, and Application to Antifouling Coatings for Filtration Membranes. *Polym. Chem.* **2013**, *4* (19), 5065−5073.
(197) Islam, M. A.; Cho, J.-Y.; Azyat, K.; Mohammadtabar, F.; Gao, F.; Serpe, M. J.; Myles, A. J.; La, Y.-H.; Sadrzadeh, M. Highly Efficient Antifouling Coating of Star-Shaped Block Copolymers with Variable Sizes of Hydrophobic Cores and Charge-Neutral Hydrophilic Arms. *ACS Appl. Polym. Mater.* **2021**, *3* (2), 1116−1134.
(198) Moore, E.; Delalat, B.; Vasani, R.; McPhee, G.; Thissen, H.; Voelcker, N. H. Surface-Initiated Hyperbranched Polyglycerol as an Ultralow-Fouling Coating on Glass, Silicon, and Porous Silicon Substrates. *ACS Appl. Mater. Interfaces* **2014**, *6* (17), 15243−15252.
(199) Le, A. N.; Liang, R.; Ji, X.; Fu, X.; Zhong, M. Random Copolymerization of Macromonomers as a Versatile Strategy to Synthesize Mixed-Graft Block Copolymers. *J. Polym. Sci.* **2021**, *59* (21), 2571−2580.
(200) Liang, R.; Xue, Y.; Fu, X.; Le, A. N.; Song, Q.; Qiang, Y.; Xie, Q.; Dong, R.; Sun, Z.; Osuji, C. O.; Johnson, J. A.; Li, W.; Zhong, M. Hierarchically Engineered Nanostructures from Compositionally

https://doi.org/10.1021/jacsau.3c00081
JACS Au 2023, 3, 1284−1300

Anisotropic Molecular Building Blocks. *Nat. Mater.* **2022**, *21* (12), 1434−1440.
(201) Liang, R.; Song, Q.; Li, R.; Le, A. N.; Fu, X.; Xue, Y.; Ji, X.; Li, W.; Zhong, M. Rapid Access to Diverse Multicomponent Hierarchical Nanostructures from Mixed-Graft Block Copolymers. *Angew. Chem., Int. Ed.* **2022**, *61* (41), e202210067.
(202) Siegers, C.; Biesalski, M.; Haag, R. Self-Assembled Monolayers of Dendritic Polyglycerol Derivatives on Gold That Resist the Adsorption of Proteins. *Chem. − Eur. J.* **2004**, *10* (11), 2831−2838.
(203) Kainthan, R. K.; Janzen, J.; Levin, E.; Devine, D. V.; Brooks, D. E. Biocompatibility Testing of Branched and Linear Polyglycidol. *Biomacromolecules* **2006**, *7* (3), 703−709.
(204) Saenz de Jubera, A. M.; Gao, Y.; Moore, J. S.; Cahill, D. G.; Mariñas, B. J. Enhancing the Performance of Nanofiltration Membranes by Modifying the Active Layer with Aramide Dendrimers. *Environ. Sci. Technol.* **2012**, *46* (17), 9592−9599.
(205) Gao, Y.; de Jubera, A. M. S.; Mariñas, B. J.; Moore, J. S. Nanofiltration Membranes with Modified Active Layer Using Aromatic Polyamide Dendrimers. *Adv. Funct. Mater.* **2013**, *23* (5), 598−607.
(206) Wang, L.; Ji, S.; Wang, N.; Zhang, R.; Zhang, G.; Li, J.-R. One-Step Self-Assembly Fabrication of Amphiphilic Hyperbranched Polymer Composite Membrane from Aqueous Emulsion for Dye Desalination. *J. Membr. Sci.* **2014**, *452*, 143−151.
(207) Joseph, N.; Thomas, J.; Ahmadiannamini, P.; Van Gorp, H.; Bernstein, R.; De Feyter, S.; Smet, M.; Dehaen, W.; Hoogenboom, R.; Vankelecom, I. F. J. Ultrathin Single Bilayer Separation Membranes Based on Hyperbranched Sulfonated Poly(Aryleneoxindole). *Adv. Funct. Mater.* **2017**, *27* (9), 1605068.
(208) Park, H. B.; Kamcev, J.; Robeson, L. M.; Elimelech, M.; Freeman, B. D. Maximizing the Right Stuff: The Trade-off between Membrane Permeability and Selectivity. *Science* **2017**, *356* (6343), eaab0530.
(209) Sun, S. P.; Hatton, T. A.; Chung, T.-S. Hyperbranched Polyethyleneimine Induced Cross-Linking of Polyamide−imide Nanofiltration Hollow Fiber Membranes for Effective Removal of Ciprofloxacin. *Environ. Sci. Technol.* **2011**, *45* (9), 4003−4009.
(210) Chiang, Y.-C.; Hsub, Y.-Z.; Ruaan, R.-C.; Chuang, C.-J.; Tung, K.-L. Nanofiltration Membranes Synthesized from Hyperbranched Polyethyleneimine. *J. Membr. Sci.* **2009**, *326* (1), 19−26.
(211) Wei, X.-Z.; Zhu, L.-P.; Deng, H.-Y.; Xu, Y.-Y.; Zhu, B.-K.; Huang, Z.-M. New Type of Nanofiltration Membrane Based on Crosslinked Hyperbranched Polymers. *J. Membr. Sci.* **2008**, *323* (2), 278−287.
(212) Sun, S. P.; Hatton, T. A.; Chan, S. Y.; Chung, T.-S. Novel Thin-Film Composite Nanofiltration Hollow Fiber Membranes with Double Repulsion for Effective Removal of Emerging Organic Matters from Water. *J. Membr. Sci.* **2012**, *401−402*, 152−162.
(213) Wei, X.; Kong, X.; Yang, J.; Zhang, G.; Chen, J.; Wang, J. Structure Influence of Hyperbranched Polyester on Structure and Properties of Synthesized Nanofiltration Membranes. *J. Membr. Sci.* **2013**, *440*, 67−76.
(214) Büning, J.; Frost, I.; Okuyama, H.; Lempke, L.; Ulbricht, M. β-Cyclodextrin-Based Star Polymers for Membrane Surface Functionalization: Covalent Grafting via "Click" Chemistry and Enhancement of Ultrafiltration Properties. *J. Membr. Sci.* **2020**, *596*, 117610.
(215) Jo, J. H.; Shin, S. S.; Jeon, S.; Park, S.-J.; Park, H.; Park, Y.-I.; Lee, J.-H. Star Polymer-Assembled Adsorptive Membranes for Effective Cr(VI) Removal. *Chem. Eng. J.* **2022**, *449*, 137883.
(216) Jeon, S.; Park, C. H.; Park, S.-H.; Shin, M. G.; Kim, H.-J.; Baek, K.-Y.; Chan, E. P.; Bang, J.; Lee, J.-H. Star Polymer-Assembled Thin Film Composite Membranes with High Separation Performance and Low Fouling. *J. Membr. Sci.* **2018**, *555*, 369−378.
(217) Vollprecht, M.; Dieterle, F.; Busche, S.; Gauglitz, G.; Eichhorn, K.-J.; Voit, B. Quantification of Quaternary Mixtures of Low Alcohols in Water: Temporal-Resolved Measurements with Microporous and Hyperbranched Polymer Sensors for Reduction of Sensor Number. *Anal. Chem.* **2005**, *77* (17), 5542−5550.
(218) Dermody, D. L.; Peez, R. F.; Bergbreiter, D. E.; Crooks, R. M. Chemically Grafted Polymeric Filters for Chemical Sensors: Hyperbranched Poly(Acrylic Acid) Films Incorporating β-Cyclodextrin Receptors and Amine-Functionalized Filter Layers. *Langmuir* **1999**, *15* (3), 885−890.
(219) Liu, Y.; Xu, P.; Yu, H.; Zuo, G.; Cheng, Z.; Lee, D.-W.; Li, X. Hyper-Branched Sensing Polymer Directly Constructed on a Resonant Micro-Cantilever for the Detection of Trace Chemical Vapor. *J. Mater. Chem.* **2012**, *22* (34), 18004−18009.
(220) Huang, T.; Hou, Z.; Xu, Q.; Huang, L.; Li, C.; Zhou, Y. Polymer Vesicle Sensor for Visual and Sensitive Detection of SO2 in Water. *Langmuir* **2017**, *33* (1), 340−346.
(221) Hou, Z.; Huang, T.; Cai, C.; Resheed, T.; Yu, C.; Zhou, Y.; Yan, D. Polymer Vesicle Sensor through the Self-Assembly of Hyperbranched Polymeric Ionic Liquids for the Detection of SO2 Derivatives. *Chin. J. Polym. Sci.* **2017**, *35* (5), 602−610.
(222) Zhou, Q.; Ma, J.; Dong, S.; Li, X.; Cui, G. Intermolecular Chemistry in Solid Polymer Electrolytes for High-Energy-Density Lithium Batteries. *Adv. Mater.* **2019**, *31* (50), 1902029.
(223) Zhao, Q.; Stalin, S.; Zhao, C.-Z.; Archer, L. A. Designing Solid-State Electrolytes for Safe, Energy-Dense Batteries. *Nat. Rev. Mater.* **2020**, *5* (3), 229−252.
(224) Manthiram, A.; Yu, X.; Wang, S. Lithium Battery Chemistries Enabled by Solid-State Electrolytes. *Nat. Rev. Mater.* **2017**, *2* (4), 1−16.
(225) Wright, P. V. Electrical Conductivity in Ionic Complexes of Poly(Ethylene Oxide. *Br. Polym. J.* **1975**, *7* (5), 319−327.
(226) Xue, Z.; He, D.; Xie, X. Poly(Ethylene Oxide)-Based Electrolytes for Lithium-Ion Batteries. *J. Mater. Chem. A* **2015**, *3* (38), 19218−19253.
(227) Ji, X.; Cao, M.; Fu, X.; Liang, R.; Le, A. N.; Zhang, Q.; Zhong, M. Efficient Room-Temperature Solid-State Lithium Ion Conductors Enabled by Mixed-Graft Block Copolymer Architectures. *Giant* **2020**, *3*, 100027.
(228) Bates, C. M.; Chang, A. B.; Momčilović, N.; Jones, S. C.; Grubbs, R. H. ABA Triblock Brush Polymers: Synthesis, Self-Assembly, Conductivity, and Rheological Properties. *Macromolecules* **2015**, *48* (14), 4967−4973.
(229) Bates, C. M.; Chang, A. B.; Schulze, M. W.; Momčilović, N.; Jones, S. C.; Grubbs, R. H. Brush Polymer Ion Gels. *J. Polym. Sci., Part B: Polym. Phys.* **2016**, *54* (2), 292−300.
(230) Xia, D. W.; Soltz, D.; Smid, J. Conductivities of Solid Polymer Electrolyte Complexes of Alkali Salts with Polymers of Methoxypolyethyleneglycol Methacrylates. *Solid State Ion.* **1984**, *14* (3), 221−224.
(231) Bannister, D. J.; Davies, G. R.; Ward, I. M.; McIntyre, J. E. Ionic Conductivities of Poly(Methoxy Polyethylene Glycol Monomethacrylate) Complexes with LiSO3CH3. *Polymer* **1984**, *25* (11), 1600−1602.
(232) Li, S.; Jiang, K.; Wang, J.; Zuo, C.; Jo, Y. H.; He, D.; Xie, X.; Xue, Z. Molecular Brush with Dense PEG Side Chains: Design of a Well-Defined Polymer Electrolyte for Lithium-Ion Batteries. *Macromolecules* **2019**, *52* (19), 7234−7243.
(233) Blonsky, P. M.; Shriver, D. F.; Austin, P.; Allcock, H. R. Polyphosphazene Solid Electrolytes. *J. Am. Chem. Soc.* **1984**, *106* (22), 6854−6855.
(234) Sun, J.; Stone, G. M.; Balsara, N. P.; Zuckermann, R. N. Structure−Conductivity Relationship for Peptoid-Based PEO−Mimetic Polymer Electrolytes. *Macromolecules* **2012**, *45* (12), 5151−5156.
(235) Zhang, Y.; Costantini, N.; Mierzwa, M.; Pakula, T.; Neugebauer, D.; Matyjaszewski, K. Super Soft Elastomers as Ionic Conductors. *Polymer* **2004**, *45* (18), 6333−6339.
(236) Rosenbach, D.; Mödl, N.; Hahn, M.; Petry, J.; Danzer, M. A.; Thelakkat, M. Synthesis and Comparative Studies of Solvent-Free Brush Polymer Electrolytes for Lithium Batteries. *ACS Appl. Energy Mater.* **2019**, *2* (5), 3373−3388.
(237) Jannasch, P. Synthesis of Novel Aggregating Comb-Shaped Polyethers for Use as Polymer Electrolytes. *Macromolecules* **2000**, *33* (23), 8604−8610.

https://doi.org/10.1021/jacsau.3c00081
JACS Au 2023, 3, 1284−1300

(238) Li, J.; Lin, Y.; Yao, H.; Yuan, C.; Liu, J. Tuning Thin-Film Electrolyte for Lithium Battery by Grafting Cyclic Carbonate and Combed Poly(Ethylene Oxide) on Polysiloxane. *ChemSusChem* **2014**, *7* (7), 1901−1908.
(239) Zhou, M.; Liu, R.; Jia, D.; Cui, Y.; Liu, Q.; Liu, S.; Wu, D. Ultrathin Yet Robust Single Lithium-Ion Conducting Quasi-Solid-State Polymer-Brush Electrolytes Enable Ultralong-Life and Dendrite-Free Lithium-Metal Batteries. *Adv. Mater.* **2021**, *33* (29), 2100943.
(240) Jing, B.; Wang, X.; Shi, Y.; Zhu, Y.; Gao, H.; Fullerton-Shirey, S. K. Combining Hyperbranched and Linear Structures in Solid Polymer Electrolytes to Enhance Mechanical Properties and Room-Temperature Ion Transport. *Front. Chem.* **2021**, *9*, 563864.
(241) Lee, S.-I.; Schömer, M.; Peng, H.; Page, K. A.; Wilms, D.; Frey, H.; Soles, C. L.; Yoon, D. Y. Correlations between Ion Conductivity and Polymer Dynamics in Hyperbranched Poly(Ethylene Oxide) Electrolytes for Lithium-Ion Batteries. *Chem. Mater.* **2011**, *23* (11), 2685−2688.
(242) Peng, Y.; Liu, H.; Zhang, X. Star Polystyrene-b-Hyperbranched Polyglycidol: Synthesis and Ionic Conductivity. *J. Polym. Sci. Part Polym. Chem.* **2009**, *47* (3), 949−958.
(243) Xinling, W.; Jianjun, C.; Ling, H.; Xiaozhen, T. Synthesis and Ionic Conductivity of Hyperbranched Poly(Glycidol). *J. Polym. Sci., Part B: Polym. Phys.* **2001**, *39* (19), 2225−2230.
(244) Shim, J.; Kim, D.-G.; Lee, J. H.; Baik, J. H.; Lee, J.-C. Synthesis and Properties of Organic/Inorganic Hybrid Branched-Graft Copolymers and Their Application to Solid-State Electrolytes for High-Temperature Lithium-Ion Batteries. *Polym. Chem.* **2014**, *5* (10), 3432−3442.
(245) Wang, A.; Xu, H.; Zhou, Q.; Liu, X.; Li, Z.; Gao, R.; Wu, N.; Guo, Y.; Li, H.; Zhang, L. A New All-Solid-State Hyperbranched Star Polymer Electrolyte for Lithium Ion Batteries: Synthesis and Electrochemical Properties. *Electrochim. Acta* **2016**, *212*, 372−379.
(246) Marzantowicz, M.; Dygas, J. R.; Krok, F.; Tomaszewska, A.; Florjańczyk, Z.; Zygadło-Monikowska, E.; Lapienis, G. Star-Branched Poly(Ethylene Oxide) LiN(CF3SO2)2: A Promising Polymer Electrolyte. *J. Power Sources* **2009**, *194* (1), 51−57.
(247) Shibuya, Y.; Tatara, R.; Jiang, Y.; Shao-Horn, Y.; Johnson, J. A. Brush-First ROMP of Poly(Ethylene Oxide) Macromonomers of Varied Length: Impact of Polymer Architecture on Thermal Behavior and Li+ Conductivity. *J. Polym. Sci. Part Polym. Chem.* **2019**, *57* (3), 448−455.
(248) Niitani, T.; Amaike, M.; Nakano, H.; Dokko, K.; Kanamura, K. Star-Shaped Polymer Electrolyte with Microphase Separation Structure for All-Solid-State Lithium Batteries. *J. Electrochem. Soc.* **2009**, *156* (7), A577.
(249) Li, N.; Wang, L.; He, X.; Wan, C.; Jiang, C. Synthesis of Star Macromolecules for Solid Polymer Electrolytes. *Ionics* **2008**, *14* (5), 463−467.
(250) Kim, D.-G.; Sohn, H.-S.; Kim, S.-K.; Lee, A.; Lee, J.-C. Star-Shaped Polymers Having Side Chain Poss Groups for Solid Polymer Electrolytes; Synthesis, Thermal Behavior, Dimensional Stability, and Ionic Conductivity. *J. Polym. Sci. Part Polym. Chem.* **2012**, *50* (17), 3618−3627.
(251) Miao, L.; Song, Z.; Zhu, D.; Li, L.; Gan, L.; Liu, M. Recent Advances in Carbon-Based Supercapacitors. *Mater. Adv.* **2020**, *1* (5), 945−966.
(252) Wu, D.; Xu, F.; Sun, B.; Fu, R.; He, H.; Matyjaszewski, K. Design and Preparation of Porous Polymers. *Chem. Rev.* **2012**, *112* (7), 3959−4015.
(253) Yang, Z.; Ren, J.; Zhang, Z.; Chen, X.; Guan, G.; Qiu, L.; Zhang, Y.; Peng, H. Recent Advancement of Nanostructured Carbon for Energy Applications. *Chem. Rev.* **2015**, *115* (11), 5159−5223.
(254) Zhong, M.; Kim, E. K.; McGann, J. P.; Chun, S.-E.; Whitacre, J. F.; Jaroniec, M.; Matyjaszewski, K.; Kowalewski, T. Electrochemically Active Nitrogen-Enriched Nanocarbons with Well-Defined Morphology Synthesized by Pyrolysis of Self-Assembled Block Copolymer. *J. Am. Chem. Soc.* **2012**, *134* (36), 14846−14857.
(255) Wang, H.; Shao, Y.; Mei, S.; Lu, Y.; Zhang, M.; Sun, J.; Matyjaszewski, K.; Antonietti, M.; Yuan, J. Polymer-Derived Heteroatom-Doped Porous Carbon Materials. *Chem. Rev.* **2020**, *120* (17), 9363−9419.
(256) Lin, X.; Xie, G.; Liu, S.; Martinez, M. R.; Wang, Z.; Lou, H.; Fu, R.; Wu, D.; Matyjaszewski, K. Fabrication of Porous Nanonetwork-Structured Carbons from Well-Defined Cylindrical Molecular Bottlebrushes. *ACS Appl. Mater. Interfaces* **2019**, *11* (20), 18763−18769.
(257) Fei, H.-F.; Li, W.; Bhardwaj, A.; Nuguri, S.; Ribbe, A.; Watkins, J. J. Ordered Nanoporous Carbons with Broadly Tunable Pore Size Using Bottlebrush Block Copolymer Templates. *J. Am. Chem. Soc.* **2019**, *141* (42), 17006−17014.
(258) Yuan, R.; Kopeć, M.; Xie, G.; Gottlieb, E.; Mohin, J. W.; Wang, Z.; Lamson, M.; Kowalewski, T.; Matyjaszewski, K. Mesoporous Nitrogen-Doped Carbons from PAN-Based Molecular Bottlebrushes. *Polymer* **2017**, *126*, 352−359.
(259) Weber, A. Z.; Mench, M. M.; Meyers, J. P.; Ross, P. N.; Gostick, J. T.; Liu, Q. Redox Flow Batteries: A Review. *J. Appl. Electrochem.* **2011**, *41* (10), 1137.
(260) Ponce de León, C.; Frías-Ferrer, A.; González-García, J.; Szánto, D. A.; Walsh, F. C. Redox Flow Cells for Energy Conversion. *J. Power Sources* **2006**, *160* (1), 716−732.
(261) Rohland, P.; Schröter, E.; Nolte, O.; Newkome, G. R.; Hager, M. D.; Schubert, U. S. Redox-Active Polymers: The Magic Key towards Energy Storage − a Polymer Design Guideline Progress in Polymer Science. *Prog. Polym. Sci.* **2022**, *125*, 101474.
(262) Sukegawa, T.; Masuko, I.; Oyaizu, K.; Nishide, H. Expanding the Dimensionality of Polymers Populated with Organic Robust Radicals toward Flow Cell Application: Synthesis of TEMPO-Crowded Bottlebrush Polymers Using Anionic Polymerization and ROMP. *Macromolecules* **2014**, *47* (24), 8611−8617.
(263) Staudinger, H.; Ochiai, E. Über hochpolymere Verbindungen: 57. Mitteilling. Viscositätsmessungen an Lösungen von Fadenmolekülen. *Z. Für Phys. Chem.* **1932**, *158A* (1), 35−55.
(264) Teator, A. J.; Varner, T. P.; Knutson, P. C.; Sorensen, C. C.; Leibfarth, F. A. 100th Anniversary of Macromolecular Science Viewpoint: The Past, Present, and Future of Stereocontrolled Vinyl Polymerization. *ACS Macro Lett.* **2020**, *9* (11), 1638−1654.
(265) Zhang, X.; Lin, F.; Cao, M.; Zhong, M. Rare Earth−Cobalt Bimetallic Catalysis Mediates Stereocontrolled Living Radical Polymerization of Acrylamides. *Nat. Synth.* **2023**, DOI: 10.1038/s44160-023-00311-9.
(266) Poelma, J. E.; Ono, K.; Miyajima, D.; Aida, T.; Satoh, K.; Hawker, C. J. Cyclic Block Copolymers for Controlling Feature Sizes in Block Copolymer Lithography. *ACS Nano* **2012**, *6* (12), 10845−10854.
(267) Bielawski, C. W.; Benitez, D.; Grubbs, R. H. An "Endless" Route to Cyclic Polymers. *Science* **2002**, *297* (5589), 2041−2044.
(268) Culkin, D. A.; Jeong, W.; Csihony, S.; Gomez, E. D.; Balsara, N. P.; Hedrick, J. L.; Waymouth, R. M. Zwitterionic Polymerization of Lactide to Cyclic Poly(Lactide) by Using N-Heterocyclic Carbene Organocatalysts. *Angew. Chem.* **2007**, *119* (15), 2681−2684.
(269) Kapnistos, M.; Lang, M.; Vlassopoulos, D.; Pyckhout-Hintzen, W.; Richter, D.; Cho, D.; Chang, T.; Rubinstein, M. Unexpected Power-Law Stress Relaxation of Entangled Ring Polymers. *Nat. Mater.* **2008**, *7* (12), 997−1002.
(270) Vagias, A.; Nelson, A.; Wang, P.; Reitenbach, J.; Geiger, C.; Kreuzer, L. P.; Saerbeck, T.; Cubitt, R.; Benetti, E. M.; Müller-Buschbaum, P. The Topology of Polymer Brushes Determines Their Nanoscale Hydration. *Macromol. Rapid Commun.* **2023**, 2300035.
(271) Romio, M.; Trachsel, L.; Morgese, G.; Ramakrishna, S. N.; Spencer, N. D.; Benetti, E. M. Topological Polymer Chemistry Enters Materials Science: Expanding the Applicability of Cyclic Polymers. *ACS Macro Lett.* **2020**, *9* (7), 1024−1033.
(272) Choi, S.; Kwon, T.; Coskun, A.; Choi, J. W. Highly Elastic Binders Integrating Polyrotaxanes for Silicon Microparticle Anodes in Lithium Ion Batteries. *Science* **2017**, *357* (6348), 279−283.

https://doi.org/10.1021/jacsau.3c00081
JACS Au 2023, 3, 1284−1300